*ejpmr, 2022, 9(7), 321-344*

SJIF Impact Factor 6.222

EUROPEAN JOURNAL OF PHARMACEUTICAL AND MEDICAL RESEARCH

www.ejpmr.com

Research Article

ISSN 2394-3211

EJPMR

# FORMULATION AND *IN VITRO* & *IN VIVO* EVALUATION OF RISPERIDONE-LOADED BIODEGRADABLE PLGA NANOPARTICLES FOR ENHANCED BRAIN TARGETING

**Ms. Priti Deshmukh* and Dr. Abhay Dharamsi**

Parul Institute of Pharmacy, Faculty of Pharmacy, Parul University, Waghodia, Vadodara, Gujarat, India-391 760.

***Corresponding Author: Ms. Priti Deshmukh**

Parul Institute of Pharmacy, Faculty of Pharmacy, Parul University, Waghodia, Vadodara, Gujarat, India-391 760.

**Article Received on 25/04/2022** **Article Revised on 15/05/2022** **Article Accepted on 05/06/2022**

## ABSTRACT

Delivering drugs across the BBB is one of the promising applications of nanotechnology in clinical neuroscience. Nanoparticles could potentially carry out multiple tasks in a predefined sequence, which is very important in the delivery of drugs across the Blood-Brain Barrier. PLGA nanoparticles were prepared by using the Solvent Displacement Method or Nanoprecipitation Technique and by using different concentrations of drug to excipient ratio, PLGA [75:25], Poloxamer-188, Acetone, water, and manufacturing attributes. The nanoparticle formulations were characterized for particle size, polydispersity index (PDI), Zeta-potential, Entrapment efficiency, DSC, XRD, and SEM studies. Optimization was performed by varying parameters like an organic solvent, drug to polymer ratio, types of surfactant, and concentration of surfactant was taken into consideration. The particle size of optimized batches was found in the range of 131 to 133 nm, with the entrapment efficiency found in the range of 88.28 to 89.87%. Entrapment efficiency was carried out by using the Sephadex G-25 column. In vitro, drug release studies of Risperidone from nanoparticles were determined using the Dialysis bag diffusion technique at a regular interval throughout 72hrs. The *in-vivo* drug distribution studies were performed by Gamma Scintigraphy. Balb/c mice were injected with the $^{99m}$Tc-labelled complex of Risperidone-loaded nanoparticles measured for radioactivity in the brain and also in different organs by a Gamma-ray spectrometer. Risperidone in the brain was relatively 3-fold higher than plain Risperidone solution in 1 hr, followed by 3.2- fold in 4 hrs and 4.91- fold higher after 12 hrs.

**KEYWORDS:** Risperidone, PLGA Nanoparticles, Poloxamer-188, Nanoprecipitation Technique, Gamma Scintigraphy, Gamma-ray spectrometer.

## INTRODUCTION

The word "schizophrenia" is less than 100 years old. However, the disease was first identified as a discrete mental illness by Dr. Emile Kraepelin in 1887 and the illness itself is generally believed to have accompanied mankind through its history.[1] The inevitable inexactitudes of this emerging science continued with the dawn of the 20th Century, when in 1908 Eugen Bleuler criticized the use of the term dementia praecox, arguing for an absence of evidence supporting a global dementing process. It was Bleuler who first coined the divisive term 'schizophrenia' in 1912. Bleuler defined schizophrenia with his four "A's", referring to the blunted Affect (diminished emotional response to stimuli); loosening of Associations (by which he meant a disordered pattern of thought, inferring a cognitive deficit), Ambivalence (an apparent inability to make decisions, again suggesting a deficit of the integration and processing of incident and retrieved information) and Autism (a loss of awareness of external events, and a preoccupation with the self and one's own thought.[2] The Swiss psychiatrist, Eugen Bleuler was also the first to describe the symptoms as "positive" or "negative". Schizophrenia is a chronic, severe, and disabling brain disease. Approximately 1 percent of the population develops schizophrenia during their lifetime – more than 2 million Americans suffer from the illness in a given year. Although schizophrenia affects men and women with equal frequency, the disorder often appears earlier in men, usually in the late teens or early twenties, than in women, who are generally affected in the twenties to early thirties. People with schizophrenia often suffer terrifying symptoms such as hearing internal voices not heard by others, or believing that other people are reading their minds, controlling their thoughts, or plotting to harm them. These symptoms may leave them fearful and withdrawn. Their speech and behavior can be so disorganized that they may be incomprehensible or frightening to others. Available treatments can relieve many symptoms, but most people with schizophrenia continue to suffer some symptoms throughout their lives; it has been estimated that no more than one in five individuals recovers completely.[3] This is a time of hope for people with schizophrenia and their families.

Research is gradually leading to new and safer medications and unravelling the complex causes of the disease. Scientists are using many approaches from the study of molecular genetics to the study of populations to learn about schizophrenia. Methods of imaging the brain's structure and function hold the promise of new insights into the disorder. Schizophrenia is found all over the world. The severity of the symptoms and long-lasting, chronic pattern of schizophrenia often cause a high degree of disability. Medication and other treatments for schizophrenia, when used regularly and as prescribed, can help reduce and control the distressing symptoms of the illness. However, some people are not greatly helped by available side effects or may prematurely discontinue treatment because of unpleasant side effects or other reasons. Even when treatment is effective, the persisting consequence of the illness- lost opportunities, stigma, residual symptoms, and medication side effects or maybe very troubling.[4] The Blood-Brain Barrier (BBB) is permeable to small and lipophilic (fat-loving) molecules (up to 800 atomic mass units, but larger molecules are not transported across unless there is an active transported system available. Thus, this is one of the stumbling blocks for drug delivery. An additional problem is the very effective efflux system p-glycoprotein (p-gp), which pumps the drug back out of cells. Overcoming the difficulty of delivering, therapeutic agents to specific regions of the brain presents a major challenge to the treatment of most brain disorders. In its neuroprotective role, the BBB functions to hinder the delivery of many potentially important diagnostic and therapeutic agents to the brain. Therapeutic molecules and genes that might be effective in diagnosis and therapy do not cross the BBB in adequate amounts.[5] Mechanisms for drug targeting in the brain involve going either "through" or "behind" the BBB. Modalities for drug delivery through the BBB entail its disruption by osmotic means, biochemically by the use of vasoactive substances such as bradykinin, or even by localized exposure to high intensity focused ultrasound (HIFU). Other strategies, to go through the BBB may entail the use of endogenous transport systems, including carrier-mediated transporters such as glucose and amino acid carriers; receptor-mediated transcytosis for insulin or transferrin; and blocking of active efflux transporters such as p-glycoprotein (p-gp). Strategies for drug delivery behind the BBB include intracerebral implantation and convection-enhanced distribution. Researchers at UCLA have successfully manipulated nanomaterials to create a new drug-delivery system that promises to solve the challenge of the poor water solubility of today's most promising anticancer drugs and thereby increase their effectiveness. Nanomedical approaches to drug delivery center on developing nanoscale particles or molecules to improve the bioavailability of a drug. Drug delivery focuses on maximizing bioavailability both at specific places in the body and over some time. This will be achieved by molecular targeting by nanoengineered devices. It is all about targeting the molecules and delivering drugs with cell precision. Nanotechnology may also help in the transfer of drugs across the BBB. Recently, the researcher has been trying to build nanoparticles loaded with drugs to gain access through the BBB. More research is needed to determine which strategies will be most effective and how they can be improved for patients with brain tumors. The potential for using BBB opening to target specific agents in brain tumors has just begun to be explored. Delivering drugs across the BBB is one of the promising applications of nanotechnology in clinical neuroscience. Nanoparticles could potentially carry out multiple tasks in a predefined sequence, which is very important in the delivery of drugs across the Blood-Brain Barrier.[6]

**Nanoparticulate system in brain targeting**

Nanoparticles drug carriers consist of solid biodegradable particles in sizes ranging from 10 to 1000 nm. They cannot freely diffuse through the BBB and require receptor-mediated transport through brain capillary endothelium to deliver their content into the brain parenchyma. Long-circulating nanoparticles made of methoxypoly (ethylene glycol) - polylactide or poly (lactide-co-glycolide) (mPEG-PLA/PLGA) has good safety profiles and provide drug-sustained release. The availability of functionalized PEG-PLA permits the preparation of target-specific nanoparticles by conjugation of cell surface ligand. Using peptidomimetic antibodies to BBB transcytosis receptor, brain-targeted pegylated immune nanoparticles can now be synthesized that should make possible the delivery of entrapped actives into the brain parenchyma without inducing BBB permeability alteration. Among the few biodegradable polymers, polymers derived from glycolic acid and form D, L-lactic acid enantiomers are presently the most attractive compounds because of their biocompatibility and their resorbability through natural pathways. They are widely used for the preparation of biodegradable medical devices and of drug-sustained release nanoparticles, microspheres, and implants marketed in Europe, Japan, and the U.S. Degradation of PLA or PLGA occurs by autocatalytic cleavage of the ester bonds through spontaneous hydrolysis into oligomers and D, L-lactic and glycolic acid monomers. Lactate converted into pyruvate and glycolate enter the Krebs' cycle to be degraded into $CO_2$ and $H_2O$. After intravenous administration of $^{14}C$-$PLA_{18000}$ radio labelled Nanoparticles to rats, 90% of the recovered $^{14}C$ was eliminated within 25 days, among which 80% was as $CO_2$[10]. Degradation rate depends on four basic parameters: hydrolysis rate constant (depending on the molecular weight, the lactic/glycolic ratio, and the morphology), amount of water absorbed, the diffusion coefficient of the polymer fragments through the polymer matrix, and solubility of the degradation products in the surrounding aqueous medium. All of these parameters are influenced by temperature, additives (including drug molecules), pH, ionic strength, buffering capacity, size and processing history, steric hindrance, etc. Despite a higher water uptake, the PLA or PLGA

blocks of mPEG-PLA/PLGA block copolymers have similar degradation behavior. The mPEG blocks are released (10–25% within 3 days and 30–50% within 20 days at pH 7.4, 37°C) after cleavage of the ester bonds, and, in the range of molecular weights of 1000–20,000, are mainly excreted via the kidney Up to an extensive PLA/PLGA polymer degradation, nanoparticle morphology and size are generally preserved. Generally, considered biocompatible, PLA or PLGA Nanoparticles have also good CNS biocompatibility. No mortality was reported with albumin-coated nanoparticles in mice with up to a 2000 mg/kg dose. In contrast, $mPEG_{2000}$-$PLA_{30000}$ nanoparticles were shown to have a good safety profile, with no apparent signs of toxicity at the highest studied dose of 440 mg/kg in mice. Nanoparticles made of mPEG-PLA/PLGA copolymers are mainly prepared using the emulsion/solvent evaporation technique or the precipitation solvent displacement techniques. In the first method, copolymers are dissolved in an organic solvent immiscible to water (such as dichloromethane, chloroform, ethyl acetate) and emulsified in an aqueous phase generally containing an emulsifying agent (mainly polyvinyl alcohol and sodium cholate). Then the solvent is evaporated off under normal or low pressure to form nanoparticles. Hydrophobic compounds (drug or else) to be incorporated are dissolved in the organic phase. Basic methods require formulation optimization depending on the type of polymers/copolymers used their molecular weights, the compound to be incorporated, the nanoparticle size to be achieved, etc. Other less frequently used methods include the emulsion solvent diffusion in an oil phase and the salting-out process. Because of their different water solubility, the hydrophobic PLA/PLGA and hydrophilic PEG blocks of the mPEG-PLA/PLGA copolymer tend to phase-separate in the presence of water. Therefore, during the organic solvent evaporation or diffusion, the PEG moieties migrate toward the aqueous phase, whereas the hydrophobic PLA/PLGA moieties aggregate as the nanoparticle core. mPEG-PLA copolymers with relatively high PEG to PLA weight ratio (e.g., $mPEG_{5000}$-$PLA_{2000\text{-}3000}$) may self-assemble as polymeric micelles. Depending on the copolymer solubility in water, polymeric micelles may be prepared either by self-dispersion in water ($mPEG_{5000}$-$PLA_{1500\text{-}2000}$) or by the precipitation/solvent evaporation technique using a classical solvent extraction procedure ($mPEG_{5000}$-$PLA_{3000\text{-}110900}$). Basically, drug entrapment efficiency depends on the solid-state drug solubility in PLA/PLGA polymer (solid dissolution or dispersion), which is related to the polymer composition (lactic/glycolic ratio), the molecular weight, the drug-polymer interaction, and the presence of end-functional groups (ester or carboxyl). The PEG moiety has no or little effect on drug loading. Because PLA and PLGA are hydrophobic polymers, lipophilic drugs are easier to formulate (in the dissolved state) in PLA/mPEG-PLA nanoparticles, than hydro soluble ones (segregation in separate domains). Drug release from biodegradable polymeric nanoparticles depends on the Fickian diffusion through the polymer matrix and on the degradation rate of the polymer. The prediction of the release profile is complex because it results from a combined effect of various parameters: solid-state drug-polymer solubility and drug-polymer interactions, polymer degradation rate, block copolymer molecular weight, and polydispersity, PEG content and molecular weight, water uptake by nanoparticles and drug solubility in the biological medium. In most studies, *in vitro* release profiles are characterized by an initial fast release (burst) of the drug close to or at the surface followed by a sustained release. Polymeric nanoparticles are excellent carriers for delivering drugs. They protect drugs from degradation until they reach their target and provide sustained release of drugs.[1] Science Daily (Jun. 28, 2007), Researchers at the University of California, Santa Barbara have discovered that attaching polymeric nanoparticles to the surface of red blood cells dramatically increases the in vivo lifetime of the nanoparticles.[2]

**Nanoparticulate system for brain targeting**

Overcoming, the difficulty of delivering therapeutic agents to specific regions of the brain presents a major challenge to the treatment of most brain disorders. In its neuroprotective role, the Blood-Brain Barrier functions to hinder the delivery of many potentially important diagnostic and therapeutic agents to the brain.

Nanotechnology is used to deliver drugs to the brain across the Blood-Brain Barrier and may provide a significant advantage to current strategies. Intravenously (IV) injected nanoparticulate drug carriers are one attempt to realize the ‘magic bullet’ concept postulated by Ehrlich, which means to target drugs specifically to their site of action.[7] The primary advantage of Nanoparticle drug carrier technology is that nanoparticles mask the Blood-Brain Barrier limiting the characteristics of the therapeutic drug molecule. Furthermore, this system provides sustain drug release in the brain, with decreased peripheral toxicity. Nanoparticles were first developed around 1970. Nanoparticle drug carriers consist of solid colloidal particles in size ranging from 10 to 1000 nm. A nanoparticle is a microscopic particle whose size is measured in nanometres (nm).[8] They consist of macromolecular materials in which the active principle is dissolved, entrapped, or encapsulated, and/or to which the active principle is absorbed or attached. Depending on the method of preparation, nanoparticles, nanospheres, or nanocapsules can be obtained with different properties and release characteristics for the encapsulated therapeutic agent.[9]

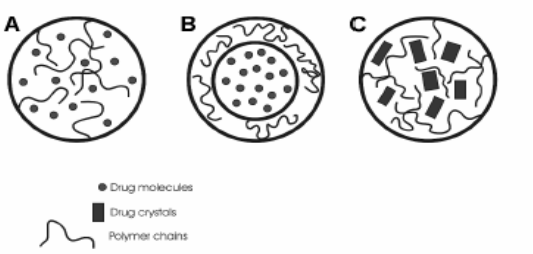


**Figure 1: Schematics of exemplary types of drug nanoparticles.**

**A.** Matrix-type nanosphere, drug molecules are evenly dispersed in the polymer matrix.
**B.** Core-shell nanocapsule, drug molecule is presented in a core covered with a polymer shell.
**C.** Matrix-type nanosphere where drug crystals are embedded in a polymer matrix.

The important technological advantages of nanoparticles used as drug carriers are high stability, high carrier capacity, the feasibility of incorporation of both hydrophilic and hydrophobic substances, and feasibility of variable routes of administration, including oral application and inhalation. Nanoparticles can also be designed to allow controlled (sustained) drug release from the matrix. Biodegradable nanoparticles of poly (d, l-lactide-co-glycolide) (PLGA) and PLGA-based polymers are widely explored as carriers for controlled delivery of macromolecular therapeutics such as proteins, peptides, vaccines, genes, antigens, growth factors Nanoparticles have a further advantage over larger microparticles as they are better suited for intravenous (IV) delivery. The smallest capillaries in the body are 5–6 µm in diameter. The size of particles being distributed into the bloodstream must be significantly smaller than 5 µm, without forming aggregates to ensure that the particles do not form an embolism.[10] Desai et al. found that nanoparticles had a 2.5fold greater uptake than 1 µm microparticles, and 6-fold greater uptakes than 10 µm microparticles.[11]

**Types of Nanoparticles**

A. Quantum Dots
 i. Nanocrystalline Silicon
 ii. Photonic
B. Crystals
 i. Liposome
 ii. Gliadin Nanoparticles
C. Polymeric Nanoparticles
 i. Solid Lipid Quantum Nanoparticles (SLN)
D. Others-gold, carbon, silver.[12]

**Brain targeting**

**Drug Delivery and the Blood-Brain Barrier**

The Blood-Brain Barrier is permeable to small and lipophilic (fat-loving) molecules (up to 800 atomic mass units), but larger molecules are not transported across unless there is an active transport system available. Thus, this is one of the stumbling blocks for drug delivery. An additional problem is the very effective drug efflux system p-glycoprotein (p-gp), which pumps the drug back out of cells.

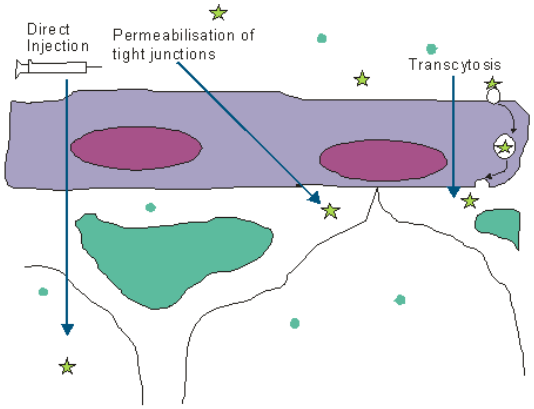


**Figure 2: Delivery across the Blood-Brain Barrier.**

**Delivery across the blood-brain barrier**

There are currently three main methods of transport across the Blood-Brain Barrier, none of which is perfect.

**1] Direct physical injection into the site of interest**

This method is highly invasive and requires specialist medical neurology teams and equipment. To date, this is still the most efficient method of delivery of drugs into the brain and is the only system used in humans.[13]

**2] Permeabilization of tight junctions**

Using either osmotic disruption or biochemical opening (RMP-7 Alkermes, vasoactive compounds – histamine). This leads to a reversible opening of the tight junction,

but is not specific and usually involves the delivery of a large bolus injection of the drug along with the permeabilization agent into the carotid artery.

**3] Enhance transcytosis across the endothelial cells**

Enhanced delivery through the endothelial cells (transcytosis) to the underlying brain cells can be achieved by increasing endocytosis (i.e. internalization of small extracellular molecules) by using liposomes or nanoparticles loaded with the drug of interest. The uptake can be further enhanced by specifically targeting the delivery system to receptors on the brain endothelium surface that are capable of receptor-mediated endocytosis. This method is more selective than the tight junction disruption, especially if brain-specific targeting technology is used, but tends to be less efficient. It also requires the discovery and development of receptor-specific ligands, which can be attached directly to the drug of interest or the drug delivery system itself.[13]

**Current strategies for brain delivery of drug**

A. Non-invasive methods
1. Enhance the lipophilicity of the drug
2. Temporary disruption of Blood-Brain Barrier

B. Invasive methods
1. Catheter with the pump system
2. Local implantation of sustained controlled release polymer

Nowadays there are two possible approaches to treating brain diseases, namely the invasive and the non-invasive approaches. The invasive approaches consist of a temporary disruption of allowing the entry of a drug into the central nervous system, or of direct drug delivery by means of intraventricular or intracerebral administrations; non-invasive approaches use intranasal delivery or colloidal drug carriers.

**2.13 Poly (D, L-lactide-*co*-glycolide)**

The biodegradable polyester family has been considered one of the few synthetic biodegradable polymers with controllable biodegradability, excellent biocompatibility, and high safety. Poly (lactic acid), poly (glycolic acid), and poly (lactic-co-glycolic acid) are the polymers of the biodegradable polyester class and have also been as called polylactide, polyglycolide, and poly (lactide-co-glycolide), respectively, according to the nomenclature system based on the source of the polymer.[14] PLGA or poly (lactic-co-glycolic acid) is an FDA-approved copolymer for its biocompatibility and biodegradability and mechanical strength.[15] PLGA is synthesized by random ring-opening co-polymerization of two different monomers, the cyclic dimmers (1, 4 dioxane-2, 5-diones) of glycolic acid (hydrophilic) and lactic acid (hydrophobic) by using a catalyst as a 2-ethylhexaanote, aluminum isopropoxide. During polymerization, successive monomeric units (of glycolic or lactic acid) are linked together in PLGA by ester linkages, thus yielding linear, aliphatic polyester as a product. Depending on the ratio of lactic to glycolic used for the polymerization, different forms of PLGA can be identified as copolymers whose composition is 75% lactic acid and 25% glycolic acid. All PLGAs are amorphous rather than crystalline and show a glass transition temperature in the range of 40-60°C. Unlike the homopolymers of lactic acid (polylactide) and glycolic acid (polyglycolide) which show poor solubility, PLGA can be dissolved by a wide range of common solvents, including chlorinated solvents, tetrahydrofuran, acetone or ethyl acetate. Depending on the ratio of lactic to glycolic [L: G] used for the polymerization, different forms of PLGA [PLGA50:50, PLGA 65:35, PLGA 75:25, PLGA 85:15].[16]

Focus on developing nanoparticles encapsulating therapeutic drugs in controlled release applications due to their advantages over the conventional devices that include extended drug release rates up to days, weeks, or months, in addition to their biocompatibility, biodegradability, and ease of administration via injection.[17] The small fraction of water absorbed resulted in polymer degradation.[17,18]

The most widely used PLGA composition of 50:50 has the fastest biodegradation rate of the d, l-lactide-glycolide polymers that degrade in about 50–60 days. Other combinations viz., 65:35, 75:25, and 80:20 have progressively longer *in vivo* life-times.[19] Amorphous polymers are characterized by glass transition temperature ($T_g$), which is the transition point between a highly viscous brittle structure called glass and a less viscous, more mobile, rubbery state. The rubbery state (above the $T_g$), represents a liquid-like structure with high molecular mobility and is thus more prone to physical and chemical changes than the glassy state. Glass transition temperature, ($T_g$) is another important parameter determining the physical strength of the delivery system. The $T_g$ of PLGA is found in the range of 45°C to 55 °C.[20]

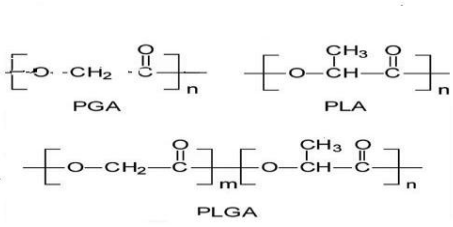


**Figure 3: Chemical structure of Polyglycolic acid, Polylactic acid, and Poly (lactic-co-glycolic acid.[21]**

**Table 1: Physical and Chemical properties of some commonly used lactide polymers.**

| Polymer Type | Inherent viscosity (dL/g) | Melting point (°C) | Glass transition temperature ($T_g$, °C) | Solubility | Specific Gravity (g/ml) |
|---|---|---|---|---|---|
| **DL-PLA** | 0.55 – 0.75 | Amorphous | 55 – 60 | 1,2,3,4,5,6 | 1.25 |
| **L-PLA** | 0.90 – 1.20 | 173 - 178 | 60 – 65 | 1,4,5 | 1.24 |
| **PGA** | 1.40 – 1.80 | 225 - 230 | 35 – 40 | 5 | 1.53 |
| **PLGA 50:50** | 0.55 – 0.75 | Amorphous | 45 – 50 | 1,2,3,4,5,6 | 1.34 |
| **PLGA 65:35** | 0.55 – 0.75 | Amorphous | 45 – 50 | 1,2,3,4,5,6 | 1.30 |
| **PLGA 75:25** | 0.55 – 0.75 | Amorphous | 50 – 55 | 1,2,3,4,5,6 | 1.30 |
| **PLGA 85:15** | 0.55 – 0.75 | Amorphous | 50 - 55 | 1,2,3,4,5,6 | 1.27 |

1 = Methylene Chloride, 2 = Tetrahydrofuran, 3 = Ethyl acetate, 4 = Chloroform, 5 = Hexafluroisopropanol, 6 = Acetone

To add hydrophilic and other physicochemical properties, poly (ethylene glycol) (PEG) has been incorporated into the biodegradable polyesters. PEG is a non-toxic, water-soluble polymer with proven biocompatibility. Block copolymers consisting of a hydrophobic polyester segment and a hydrophilic PEG segment have attracted large attention due to their biodegradability, biocompatibility, and tailor-made properties.[22]

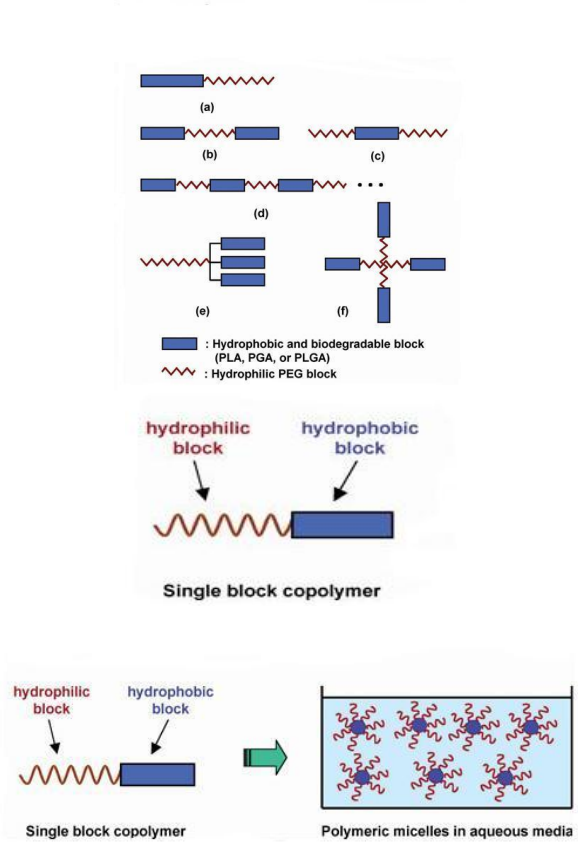


**Figure 4: Various kinds of block copolymers.**

Various kinds of block copolymers have been developed to date and can be classified according to their block structure as AB diblock, ABA, or BAB, triblock, multi-block, branched block, star-shaped block, and graft block copolymers, in which A is a hydrophobic block made up of biodegradable polyesters and B is a hydrophilic PEG block.[22,23] There are four major established suppliers of GMP-grade PLGA polymers in the market. These include Purac (Trade name: Purasorb); Absorbable Polymers International, a wholly-owned international subsidiary of Durect Corporation (Trade name: Lactel); Alkermes (Trade name: Medisorb); Boehringer Ingelheim (Trade Name: Resomer). Other newer suppliers include Absorbable Polymer Technologies (US) and smaller manufacturers catering to the local niche markets worldwide.[24]

**Table 2: The list of FDA approved drug delivery products of PLGA polymer.**

| Product name | Active ingredient | Company | Application |
|---|---|---|---|
| Lupron Depot® | Leuprolide acetate | TAP | Prostate cancer |
| Nutropin Depot® | Growth hormone | Genetech | Pediatric growth hormone deficiency |
| Suprecur® MP | Buserelin acetate | Aventis | Prostate cancer |
| Decapeptyl® | Triptorelin pamoate | Ferring | Prostate cancer |
| Sandostatin LAR® Depot | Octreotide acetate | Novartis | Acromegaly |
| Somatuline® LA | Lanreotide | Ipsen | Acromegaly |
| Trelstar™ Depot | Triptorelin pamoate | Pfizer | Prostate cancer |
| Arestin® | Minocycline | Orapharma | Periodontal disease |

**Techniques of preparation of nanoparticles**

The basis and commonly used methods for the preparation of Nanoparticles are as follows.

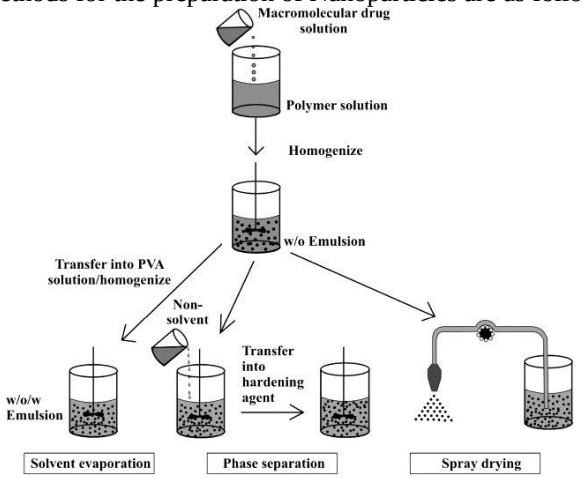


**Figure 5: Various methods of preparation of Nanoparticles: (I) Solvent evaporation, (II), Polymer phase separation, and (III) Spray drying.[24]**

**Emulsification solvent evaporation**

The most common method used for the preparation of solid, polymeric nanoparticles is the Emulsification–solvent evaporation technique. In this method, the polymer is dissolved in a water-immiscible, volatile organic solvent which is then emulsified with an aqueous phase by using an appropriate stabilizer. The organic solvent is then evaporated inducing the formation of polymer particles from the organic phase droplets. The solvent evaporation method was described by Niwa et al and has since been widely used to prepare particles from a range of polymeric materials, particularly PLA and PLGA. This technique has been successful in encapsulating hydrophobic drugs.[25] The various factors that affect the formation of the nanoparticles are the nature of the polymer, polymer molecular weight nature of organic phase, polymer concentration in the organic phase, and volume ratio of organic: aqueous phase, nature of surfactant, surfactant concentration, and molecular weight, stirring speed.[26]

The main drawback of this method, after the preparation of nanoparticles in the range of 200 nm there is a need to remove the excipients mainly in the case of organic solvents will have toxicological implications. The excess surfactant used is difficult to remove. Another limitation is that surfactant must be present for the preparation of nanoparticles to stabilize the system.[26,27]

**Double emulsion solvent evaporation method**

The emulsion solvent evaporation technique was further modified and a double emulsion (or multiple emulsion) of water in oil in water type has been further followed by evaporation of the organic solvent and resulting in the formation of nanoparticles. The formed nanoparticles are then further recovered by ultracentrifugation, washed repeatedly by the buffer, and lyophilized. Typically, Bovine serum albumin (BSA) and PLGA are dissolved separately in the aqueous and organic phase respectively (containing the stabilizer) and subjected to ultrasonication to yield water–in-oil-in water [W1/ O/ W2] double emulsion. Then organic phase is allowed to evaporate at atmospheric pressure and then at reduced pressure to yield nanoparticles.[28]

**Interfacial polymerization methods**

This method was first described by Fessi et al. nanoparticles can also be polymerized by interfacial polymerization and denaturation/ desolvation for drug delivery to the CNS. Like emulsion polymerization, in interfacial polymerization, the monomers are used to create the solution. High-torque mechanical stirring brings the aqueous and organic phases together by emulsification or homogenization. Poly (alkyl cyanoacrylate) NPs are polymerized by this method. In addition, denaturation and desolvation have been used to produce polymeric NPs. Decreased miscibility of organic

solvents with water is associated with an increase in their resultant interfacial tension and thus increases the size of the nanoparticles. The higher the viscosity of the organic phase, the greater will be surface tension, and ultimately the particle size of the nanoparticles will be increased. An increase in molecular weight of polymers is associated with a decrease in the number of ends carboxyl groups and hence lowers the Zeta potential of the resulting particles. Additives present in the formulation may also significantly affect this surface charge Pluronic F-68, PVA-like surfactants may be added to improve steric stability of nanoparticles.[29]

**Salting out**

Bindschaedler and co-workers first described this technique in 1988. The technique involves an emulsification technique in which one has to avoid the use of chlorinated solvents. A saturated salt solution containing a stabilizing agent such as PVA is added under stirring to an acetone solution of the polymer. An o/w emulsion forms as the salt prevents the water and acetone mixing. Sufficient water is then added to allow the acetone to diffuse into the external aqueous phase and induce nanoparticle formation. By considering the entrapment efficiency of nanoparticles this method is most suitable for water-insoluble drugs. Salts permeate biological systems and are crucial for life.[31]

**Supercritical fluids technology**

Recently the field of supercritical fluids has been investigated as an approach to the preparation of sub-micron-sized particles.[32] The rapid expansion of supercritical solutions consists in saturating a supercritical fluid with the substrate(s), then depressurizing this solution through a heated nozzle into a low-pressure chamber in order to cause extremely rapid nucleation of the substrate(s) in form of very small particles or fibers, or films when the jet is directed against a surface that is collected from the gaseous stream. The major merits of these processes include the production of organic solvent-free particles, mild operating temperatures for processing biological materials, and easier micro-encapsulation of drugs for controlled release of the therapeutic agents.[34,33] Unfortunately, none of these techniques can produce small protein particles in the sub-micron range of less than 300 nm having a very narrow size distribution. Fine particles of model compound cholesterol acetate (CA), griseofulvin (GF), and megestrol acetate (MA) were produced by extraction of the internal phase of oil-in-water emulsions using supercritical carbon dioxide.[35]

**Solvent Displacement method or nanoprecipitation technique**

This method is based on the interfacial deposition of a polymer following the displacement of a semi-polar solvent miscible from a lipophilic solution. Solvent displacement involves the use of an organic phase that is completely soluble in the external aqueous phase. The organic solvent diffuses instantaneously to the external aqueous phase, which immediate polymer precipitation due to the miscibility of both the phases. In this method, neither separation nor extraction of the solvent is required for the polymer precipitation. Polymer and drug are dissolved in a semipolar water-miscible solvent like acetone or ethanol which results in the formation of the organic phase. This organic phase is then injected into the aqueous phase, which consists of distilled water and surfactant. The organic phase is injected into the aqueous phase at the rate of 1ml/min. under magnetic stirring. The injection rate of the organic phase in the aqueous phase affects the resultant nanoparticle size. Nanoparticles are formed instantaneously by rapid solvent evaporation from the organic phase. This method is particularly useful for drugs that are slightly soluble in water. The nanoprecipitation method gave excellent entrapment efficiency with narrow particle size distribution. The difficulty in this preparation technique is the choice of drug/ polymer/ solvent/ nonsolvent system in which the nanoparticles would be formed and drug entrapment efficiency. After nanoparticle preparation, the solvent is eliminated and the free-flowing nanoparticles are obtained under reduced pressure.[36]

## MATERIALS AND METHODS

**Materials**

Risperidone was provided as a gift sample from Ranbaxy Laboratories, India. Polylactic-co-glycolic acid PLGA [75:25] with a molecular weight of 15 kD with a lactide-glycolide ratio of 75:25 and Poloxamer-188(Pluronic F-68) was provided as a gift from Sun Pharmaceutical Industries Limited, India. Acetone, Acetonitrile was used of Analytical grade for the formulation of nanoparticles. Sephadex G-25 was used for the separation of free drugs. The water implies the use of distilled water filtered through a 0.22 µm cellulose nitrate membrane. The buffers were prepared in the research laboratory of the department. All the other reagents used were of analytical grade.

**Method**

**Solvent displacement method or nanoprecipitation technique**

PLGA nanoparticles were prepared by using the Solvent Displacement Method or Nanoprecipitation Technique. The organic phase was prepared with 100 mg of PLGA [75: 25] and 10 mg of Risperidone was weighed and dissolved in 5 ml of Acetone. The Polymer and drug were allowed to dissolve in the solvent completely. The aqueous phase was prepared by dissolving the 0.2 gm of Poloxamer-188 into 20 ml of distilled water, which was previously filtered through a 0.22 µm cellulose nitrate membrane. The organic phase was then injected into the aqueous phase at the rate of 0.3 ml/min. The stirring rate was kept at 700 RPM. Then stirring was continued for 3 to 4 Hrs to remove the organic solvent completely. The resultant nanosuspension was then characterized for size analysis, Zeta-potential, and Polydispersity index. For the separation of free drugs, nanosuspension was passed

through the Sephadex G-25 column. After the separation of the free drug from the nanosuspension, the Lyophilization was carried out by using sucrose as a cryoprotectant for 24 Hrs.

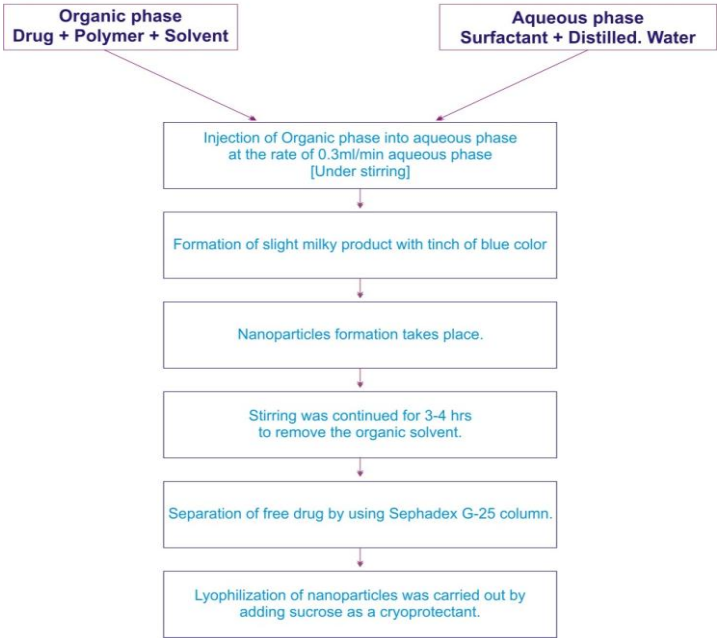


**Figure 6: Schematic diagram of the preparation of Nanoparticles by Nanoprecipitation Technique.**

***In vivo* Radiolabelling and biodistribution studies**

The Hungarian scientist Prof. George Hevesy chemist and recipient of the 1943 Nobel Prize for Chemistry. His development of isotopic tracer techniques greatly advanced his understanding of the chemical nature of life processes. The principles guiding the choice of a radioisotope for any particular application are the half-life, radiation characteristics, ease of production, and cost. The use of radioisotopes for the diagnosis and therapy of various disease conditions constitutes one of the major applications of isotopes. The radioisotopes or isotopic preparation used in medicine are called Radiopharmaceuticals. A radiopharmaceuticals product can be described as a special class of radioisotopes product a chemical formulation containing a radionuclide of adequate purity and safety suitable for oral/ intravenous administration to humans for performing an in-vitro for medical purposes. Drug deposition for intravenous formulations may be quantified using radionuclide-imaging studies. The two-dimensional (2-D) imaging method of Gamma Scintigraphy and the three-dimensional (3-D) imaging method of SPECT both normally use a gamma-emitting radionuclide, such as $^{99m}$Tc. Over time, Anger's scintillation camera evolved into modern imaging systems such as PET (positron emission tomography) and SPECT (single-photon emission computed tomography). The evolution of this technology was shaped by Anger, his colleagues, and his successors here. Their contributions include the multi-crystal whole-body scanner (1970), gated heart single gamma tomography (1974), and dynamic and gated PET (1978). Today, 160 PET cameras are operating in hospitals, and medical and research facilities worldwide. The highest resolution PET scanner in the world, the 2.6 millimeter-resolution camera was built by Budinger's colleagues Steve Derenzo and Ronald Huesman.[37,38]

**Reactor Radioisotopes (Half-life indicated)**

Bismuth-213 (46 min), Chromium-51 (28 d), Cobalt-60 (10.5 month), Copper-64 (13 Hrs), Dysprosium-165 (2 Hrs), Erbium-169 (9.4 days), Holmium-166 (26 Hrs), Iodine-125 (60 days), Iodine-131 (8 days), Iridium-192 (74 days), Iron-59 (46 days), Lutetium-177 (6.7 days), Palladium-103 (17 days), Phosphorus-32 (14 days), Potassium-42 (12 Hrs), Rhenium-186 (3.8 days), Rhenium-188 (17 Hrs), Samarium-153 (47 Hrs), Selenium-75 (120 days), Sodium-24 (15 Hrs), Strontium-89 (50 days), Xenon-133 (5 days), Ytterbium-169 (32 days), Ytterbium-177 (1.9 Hrs), Progenitor of Lu-177, Yttrium-90 (64 Hrs).

Molybdenum-99 (66 h), Used as the 'parent' in a generator to produce Technetium-99m.

$^{99}$Mo $\longrightarrow$ $^{99m}$Tc

Technetium-99m (6 h), Used in to image the skeleton and heart muscle in particular, but also for the brain, thyroid, lungs (perfusion and ventilation), liver, spleen, kidney (structure and filtration rate), gall bladder, bone marrow, salivary and lachrymal glands, heart blood pool, infection and numerous specialized medical studies.

**Common methods of separation of $^{99m}$ Tc and $^{99}$Mo**

A. Column chromatography over-acidic alumina.
B. Solvent extraction of $^{99m}$Tc with methyl ethyl ketone
C. Sublimination of Tc oxides from Mo compound

**Cyclotron Radioisotopes**

Carbon-11: Nitrogen-13: Oxygen-15: Fluorine-18: Cobalt-57 (272 d): Gallium-67 (78 h): Indium-111 (2.8 d): Iodine-123 (13 h): Krypton-81m (13 sec) from Rubidium-81 (4.6 h): Rubidium-82 (65 h): Strontium-92 (25 d): Thallium-201 (73 h).[39]

**Advantages of technetium-$^{99}$m [$^{99m}$Tc]**

The radioisotope most widely used in medicine is technetium-99m, employed in some 80% of all nuclear medicine procedures - 40,000 mCu every day. It is an isotope of the artificially produced element technetium and it has almost ideal characteristics for a nuclear medicine scan. These are:

1. The low-energy gamma rays it emits easily escape the human body and are accurately detected by a gamma camera. Once again, the radiation dose to the patient is minimized.
2. It has a half-life of 6 Hrs, which is long enough to examine metabolic processes yet short enough to minimize the radiation dose to the patient.
3. Technetium-99m decays by a process called "isomeric"; which emits gamma rays and low energy electrons. Since there is no high-energy beta emission the radiation dose to the patient is low.
4. The decay of $^{99m}$Tc is not associated with any particulate emission and hence $^{99m}$Tc radiopharmaceuticals typically containing 5-20 mCu of the isotopes can be injected safely into patients. Such large doses help in getting better quality images and thereby more information.
5. The chemistry of technetium is so versatile it can form tracers by being incorporated into a range of biologically active substances to ensure that it concentrates in the tissue or organ of interest.
6. $^{99m}$Tc can be conveniently obtained from a generator system.[40]

**Physical properties of $^{99m}$Tc**

The mapping of the actual distribution of radioactivity in the organ known as 'Scintigraphy' was initially done using rectilinear scanners. The moving detector, in this case, records the activity at each point of the organ, on a point-by-point and line-by-line basis using the electromechanical design of the device. Such an imaging procedure is a slow process and is of limited scope or utility. There are many situations in which the dynamic changes taking place in the organ are of prime interest apart from a need to probe the actual pathway following administration of the product.

The 'Gamma camera' which is the most widely used device fulfills the above requirements. It consists of a relatively large but thin crystal of NaI (TI), 400-550 mm in diameter and up to 20 mm in thickness, coupled to an array of photomultiplier tubes and associated electronic devices. The gamma camera can count the activity from the whole organ at a time and with the help of a computer gives the images of the organ on a monitor screen. In addition, tomographic capabilities by giving provision for the rotation of the gamma camera around the patient and collection of data at various angles improved the 'vision' and facilities better quantification of the radiopharmaceuticals in the Single Photon Emission Computed Tomography [SPECT] machines.[42]

**Measurement of radioactivity**

The principle involved in the measurement of radioactivity is as follows; the gamma rays emitted by the isotopes enter a stainless-steel casing and generate electrons, which are absorbed by the sodium iodide [NaI] crystal. The NaI crystal undergoes excitation and further de-excitation to produce a flash of light. This flash of light passes through an optically coupled photomultiplier tube. In the photomultiplier tube, the intensity is enhanced and passes through a pre-amplifier and linear amplifier and consequently to the pulse height analyzer. The signals are then turned and recorded in the recorder in case of a gamma camera. The gamma camera is equipped with a scalar instead of a recorder. In scalar, the signals are converted into digits in terms of counts.[42]

**Principles of radiolabelling of compounds with $^{99}$mTc**

The majority of 99mTc compounds employ the stannous chloride reduction method, which makes use of the fact that stannous chloride is one of the most powerful reducing agents. $^{99}$mTc obtained from the Mo /Tc generator is in the chemical form of $TcO_4$- or pertechnetate. While the anion has an overall negative charge of -1, the oxidation number of technetium is -7. The chelating agents commonly used to prepare 99mTc products are also anions with an overall negative charge due to the presence of N, O and P atoms, each of which has 1 or more extra pairs of electrons. These negative charges repel each other so pertechnetate will not form chelates. A reducing agent is therefore required to convert the $^{99}$mTc into an electropositive cationic form capable of binding to chelating agents. $^{99}$mTc sulfur collides and $^{99}$mTc DMSA are the only two commercially available compounds that do not use the stannous reduction method. In the reaction, the stannous ion is the reducing agent, and therefore the substances are reduced. Most soluble $^{99}$mTc compounds, excluding those containing a protein, have octahedral structures and are said to be hexa coordinated since there are typical 6 binding sites available consisting of N, O, or P atoms.[43]

**Radiolabelling of Nanoparticulate system**

Risperidone-loaded PLGA Nanoparticles were radiolabelled with $^{99m}$Tc by using stannous chloride as a reducing agent. Risperidone-loaded nanoparticles were radiolabelled as follows; 500 µlits of the formulation were taken and 50 µlits of $Sncl_2$ solution were added followed by the addition of 500 µlits of $^{99}$mTc. 100 µlits of 0.5 M sod-bi- carbonate pH as adjusted to 6.5. Then the above solution was incubated at room temperature for 15 minutes in a radiation field. The Radiolabelling efficiency of Nanoparticles formulation was determined by instant ascending thin layer chromatography [ITLC]. The ITLC strip was spotted with 10 µlit of radio-labelled

complex at 1 cm from the bottom and all it to dry for 5 min. Then allowed it to develop in 0.9% saline, Acetone, Methanol, Pyridine: Acetic acid: Water [3:5:1.5] as a mobile phase. The solvent front was allowed to reach up to a height of 10 cm from the origin. The strip was then allowed to dry completely and cut at a distance of 1 cm, and the radioactivity of each strip was measured by using a Scintillation counter. The free pertechnetate is obtained at the solvent front [at the top portion of the ITLC strip] leaving the reduced/-hydrolyzed $^{99}$mTc along with the labelled complex at the bottom. Incorporation of excess stannous chloride for reduction of $^{99}$mTc may lead to the formation of radiocolloids, which is undesirable. The radiocolloid formation was determined by Pyridine: Acetic acid: Water [3:5:1.5]. The radiocolloids remain at the bottom of the strip, while both the free pertechnetate and labelled complex migrated at the solvent front. By subtracting the migrated activity with the solvent, the net amount of $^{99}$mTc-Risperidone-loaded nanoparticles complex was calculated.

**Stability of $^{99}$mTc labelled complex in Human serum**

From the human serum stability of the radiolabelled complex in the biological environment, one can inject it into the body fluid. In vitro, human serum stability of the radiolabelled complex is an important parameter to be determined because the serum protein can chelate and bind with the $^{99}$mTc, disturbing the stability of the radiolabelled complex. In vitro serum stability was studied as follows: The radiolabelled complex of Risperidone Nanoparticles was allowed to incubate with the freshly collected human serum for 24 Hrs at 37°C. The samples were withdrawn at the regular interval upto 24 Hrs and analyzed by using ITLC, and radioactivity was measured by using a Scintillation counter.

**DTPA and Cysteine Challenging test**

These studies were performed in order to check the binding strength of $^{99}$mTc with the radiolabelled complex. In brief, fresh solutions of DTPA and Cysteine (25, 50, and 100 mM) were prepared in 0.9% saline. Five hundred microliters of the labelled preparation were treated with different concentrations of DTPA and Cysteine separately and incubated for 1 hour at 37°C. Five hundred microliters of 0.9% saline served as control. The effect of DTPA and Cysteine on the labelling efficiency of complexes was measured by ITLC-silica gel strips using Pyridine: Acetic acid: Water [3:5:1.5] as the mobile phase. In this system $^{99m}$Tc-Risperidone-loaded nanoparticles complexes remain at the origin (Rf = 0.0), while pertechnetate (Rf = 0.9 - 1.0) and all known chemical forms of $^{99m}$Tc-DTPA and $^{99m}$Tc-Cysteine complexes migrate (Rf = 0.7 - 1.0). After development, each paper strip was cut at a distance of 1 cm and each strip was counted for radioactivity in the radio-assay counter.[44,45]

**Biodistribution studies**

**Animals for biodistribution Studies**

Balb/c mice weighing ~ 25 to 30 g. were selected for the study. Quantitative biodistribution studies were performed in Balb/c (6 - 8 weeks of age). All procedures involving the use and care of animals were performed according to the guidelines of the Local Animal Ethics Committee of Bhabha Atomic Research Center [BARC], Mumbai.

**Experimental**

Quantitative biodistribution studies were performed in Balb/c mice weighing ~20 to 25gm. The biodistribution studies of radiolabelled complex Risperidone nanoparticles were performed after 1, 4, and 12 hours of post-injection, respectively. Unanesthetized animals were injected with 0.36MBq of [$^{99m}$Tc-labelled complex of Risperidone-loaded nanoparticles] via the tail vein. After 1, 4, and 12 Hrs animals were anesthetized with chloroform and at these time intervals, the blood was collected by cardiac puncture and sacrificed by decapitation. The organs were then weighed and measured for radioactivity in a gamma-ray spectrometer.[46] The radioactivity was interpreted as the percentage of injected dose per gram of organ/tissue ± SD (n= 3 for each time point).

**Determination of entrapment efficiency**

**Preparation of Sephadex G-25 column**

250 mg of Sephadex G-25 was taken and allowed to soak it with distilled water overnight. On the next day, the glass column was taken and Whatman filter paper was placed at the bottom of the column, and soaked Sephadex G-25 was added. Then this wet column was centrifuged at 1000 RPM for 5 minutes at room temperature, due to which complete removal of water from the column takes place and the packed Sephadex G-25 column was obtained.

**Determination of entrapment efficiency**

The packed Sephadex G-25 column was fixed on a stand and 2 ml of nanosuspension was passed through it. To this resultant elute obtained, 3 ml of acetonitrile was added and the UV spectroscopic absorbance was taken at 278 nm. After placing the value of absorbance into the calibration curve of the drug in acetonitrile, the Entrapment efficiency was determined.

$$\text{Entrapment efficiency (\%)} = \frac{\text{Entrapped drug}}{\text{Total drug by assay}} \times 100$$

**Optimization of Risperidone-loaded PLGA nanoparticles**

For the optimization of nanoparticles formulation, the nanoparticles were prepared by the Solvent Displacement method or Nanoprecipitation Technique. Optimization of various formulation parameters like an organic solvent, drug to polymer ratio, types of surfactant, concentration of surfactant were taken into consideration. The criteria taken for an optimum formulation were particle size, polydispersity index, Zeta-potential, and entrapment efficiency. The drug content in nanoparticles was determined by taking 1 ml of nanoparticles suspension with 9 ml of acetonitrile and the absorbance of the solution measured UV spectrophotometrically at 278 nm. The particle size, polydispersity index, and Zeta-potential were measured by the Malvern instrument. During each optimization step particle size, polydispersity index, and Zeta-potential were determined.

**Optimization of organic solvents**

In the optimization of the organic solvent, the three different solvents like methanol, acetone, and chloroform were tried.

**Table 3: Optimization of organic solvents.**

| Batch No. | Organic solvent | Particle size (nm) | P.D. I | Zeta-potential (mV) | Entrapment Efficiency % |
|---|---|---|---|---|---|
| **B1** | Methanol | 288 ± 1.9 | 0.487 ± 0.08 | -23.5 | 65.78 ± 1.45 |
| **B2** | Acetone | 158 ± 2.2 | 0.247 ± 0.06 | -30.4 | 72.42 ± 1.1 5 |
| **B3** | Chloroform | 225 ± 2.1 | 0.387 ± 0.09 | -21.6 | 61.63 ± 1.85 |

Acetone gives the particle size in the range of 158 nm with the entrapment efficiency of 72.42 ± 1.15, whereas the methanol and chloroform produce the nanoparticles in the range of 225 to 288, which are not suitable for efficient brain targeting. At the same time, entrapment efficiency was also calculated for all the experiments of the above-given solvent.

**Optimization of Drug to Polymer ratio**

**Optimization of Drug to Polymer ratio [1:5]**

In the optimization of the preparation of nanoparticles, different drug to polymer ratios were used. By using the drug to polymer ratio as 1: 5 the results obtained are as follows.

**Table 4: Optimization of Drug to Polymer ratio [1:5]**

| Batch No. | Drug: polymer | Particle size (nm) | P.D.I | Zeta-potential (mV) | Entrapment efficiency % |
|---|---|---|---|---|---|
| **B4** | 1:5 | 70 ± 1.5 | 0.246 ± 0.06 | -20.2 | 60.48 ± 1.12 |
| **B5** | 1:5 | 71 ± 1.7 | 0.245 ± 0.0.4 | -24.8 | 62.68 ±1.45 |
| **B6** | 1:5 | 72 ± 1.3 | 0.169 ± 0.07 | -19.6 | 61.75 ± 1.24 |
| **B7** | 1:5 | 70 ± 2.1 | 0.205 ± 0.03 | -26.4 | 62.41 ±1.25 |
| **B8** | 1:5 | 71 ± 2.5 | 0.198 ± 0.01 | -27.5 | 61.89 ±1.85 |

From the above results, we can conclude that by using the drug to polymer ratio as 1:5 the nanoparticles are in the range, but due to the decrease in the size of nanoparticles, the agglomeration takes place and result in the sudden increase in particles size takes place causes instability. At the same time, the entrapment efficiency of drugs in nanoparticles was found to be low in the range of 60.48 to 62.41%.

**Optimization of drug to polymer ratio [1:10]**

To obtain the nanoparticles in the required range and to increase the entrapment efficiency, a drug to polymer 1:10 was taken. The results obtained are as follows.

**Table 5: Optimization of Drug to Polymer ratio [1:10]**

| Batch No. | Drug: polymer | Particle size (nm) | P.D.I | Zeta-potential (mV) | Entrapment efficiency % |
|---|---|---|---|---|---|
| **B9** | 1:10 | 130 ± 2.2 | 0.148 ± 0.07 | -20.26 | 88.85 ± 1.14 |
| **B10** | 1:10 | 131 ± 2.4 | 0.152 ± 0.06 | -22.26 | 89.47 ± 1.36 |
| **B11** | 1:10 | 133 ± 4.4 | 0.161 ± 0.04 | -12.4 | 89.59 ± 1.21 |
| **B12** | 1:10 | 131 ± 3.6 | 0.154 ± 0.05 | -18.96 | 89.97 ± 1.54 |
| **B13** | 1:10 | 132 ± 3.8 | 0.169 ± 0.03 | -19.54 | 89.87 ± 1.36 |

From the above results we can conclude that by using the drug to polymer 1:10, the particle size, Polydispersity index, and Zeta-potential are in the range which is required for efficient brain targeting. The entrapment efficiency of nanoparticles was found in the range of 88.85 to 89.97%. The particle size was found in the range of 130 to 133 nm. P.D.I was found in the range of 0.148 to 0.169 mV.

**Optimization of drug to polymer ratio [1:15]**

By using the Drug to the polymer as 1: 15 the results obtained are as follows.

**Table 6: Optimization of Drug to Polymer ratio [1:15]**

| Batch No. | Drug: polymer | Particle size (nm) | P.D.I | Zeta-potential (mV) | Entrapment efficiency % |
|---|---|---|---|---|---|
| **B14** | 1:15 | 234 ± 1.2 | 0.282 ± 0.05 | -19.6 | 68.85 ± 1.47 |
| **B15** | 1:15 | 234 ± 1.5 | 0.255 ± 0.03 | -25.6 | 67.58 ± 1.54 |
| **B16** | 1:15 | 235 ± 2.0 | 0.241 ± 0.02 | -24.9 | 68.24 ± 1.05 |
| **B17** | 1:15 | 236 ± 1.6 | 0.265 ± 0.04 | -28.9 | 67.85 ± 1.45 |
| **B18** | 1:15 | 235 ± 2.0 | 0.246 ± 0.06 | -29.3 | 66.05 ± 1.24 |

The increase in polymer concentration produces an increased particle size, which is not suitable for brain targeting, and not a satisfactory increase in the entrapment efficiency found. Hence, for the preparation of nanoparticles, a 1:10 drug to polymer ratio was found to be suitable which produces the size of the nanoparticles in the range of 130 to 133nm, and PDI in the range of 0.148 to 0.169. The entrapment efficiency is in the range of 88.85 to 89.97%. Using the drug to polymer 1:10 performed further batches.

**Optimization of surfactants**

By using Tween-80 for Drug to polymer ratio [1:10]

**Table 7: Optimization of Tween-80 for Drug to Polymer ratio [1:10]**

| Batch No. | Tween-80 (w/v) | Drug: Polymer | Particle size (nm) | P.D.I | Zeta-potential (mV) | Entrapment Efficiency (%) |
|---|---|---|---|---|---|---|
| **B19** | 0.5 % | 1:10 | 285 ± 1.95 | 0.484 ± 0.02 | -25.6 | 42.15 ± 1.767 |
| **B20** | 1.0 % | 1:10 | 276 ± 1.98 | 0.349 ± 0.05 | -25.3 | 59.20 ± 1.018 |
| **B21** | 1.5 % | 1:10 | 271 ± 2.04 | 0.465 ± 0.03 | -24.9 | 62.28 ± 1.113 |
| **B22** | 2.0 % | 1:10 | 225 ± 2.24 | 0.425 ± 0.06 | -.19.4 | 60.48 ± 1.248 |

By using, Tween-80 as a surfactant the particle size was found in the range of 225 to 300 nm, and entrapment efficiency was found between 42.15% to 62.28%. The Zeta potential was found in the range of -19.4 to -25.6. The particle size formed by using Tween-80 was above 200 nm which is not efficient for brain targeting and hence Poloxamer-188 was further used as a surfactant.

**Optimization of Poloxamer-188 for Drug to polymer ratio [1:10]**

**Table 8: Optimization of Poloxamer-188 for Drug to Polymer ratio [1:10]**

| Batch No. | Poloxamer-188 (w/v) | Drug: polymer | Particle size (nm) | P.D.I | Zeta-potential (mV) | Entrapment efficiency % |
|---|---|---|---|---|---|---|
| **B23** | 0.5 % | 1:10 | 205 ± 1.95 | 0.304 ± 0.02 | -28.58 | 62.15 ± 1.767 |
| **B24** | 1.0 % | 1:10 | 131 ± 2.04 | 0.285 ± 0.04 | -20.74 | 88.48 ± 1.248 |
| **B25** | 1.5 % | 1:10 | 105 ± 2.04 | 0.095 ± 0.03 | -22.85 | 71.28 ± 1.113 |

Poloxamer-188 was used as a surfactant with a concentration range of 0.5%, 1%, and 1.5%. By using the 1.0% w/v of poloxamer-188, the particle size was found in the range of 131 ± 2.04 (nm) with the entrapment efficiency of 88.48%, as the conc. of Poloxamer-188 increases, particle size was found to decrease, but the entrapment efficiency was found to decrease and found in the range of 71.28 ± 1.113. As particle size for 1%w/v Poloxamer-188 was found in the range with high entrapment efficiency and hence further batches were carried out by using Drug: Polymer [1:10] with 1% w/v poloxamer-188.

The optimized batches are further formulated by using the drug to polymer ratio of 1:10 and the Poloxamer-188 concentration of 1%.

**Table 9: Optimize batches for nanoparticles containing a 1:10 drug to polymer ratio with 1% Poloxamer-188.**

| Batch No. | Poloxamer-188 (w/v) | Drug: polymer | Particle size (nm) | P.D.I | Zeta Potential (mV) | Entrapment efficiency % |
|---|---|---|---|---|---|---|
| **B26** | 1% | 1:10 | 132 ±1.26 | 0.094±0.02 | -19.3 | 88.28±1.87 |
| **B27** | 1% | 1:10 | 131 ±1.47 | 0.090±0.08 | -23.5 | 89.89±2.01 |
| **B28** | 1% | 1:10 | 132 ±1.36 | 0.102±0.04 | -20.0 | 89.47±1.65 |
| **B29** | 1% | 1:10 | 132 ±1.54 | 0.094±0.06 | -25.4 | 88.34±1.54 |
| **B30** | 1% | 1:10 | 133 ±1.36 | 0.152±0.05 | -29.6 | 89.12±1.85 |

The particle size of the above batches is found to be in the range of 131 to 133 nm which is better suited for brain targeting, at the same time Polydispersity index was found in the range of 0.094 to 0.152. Zeta-potential in the range of -19.3 to -29.6 mV. The entrapment efficiency was found in the range of 88.28 to 89.87%.

As the batches were found in the range, which is suitable for efficient brain targeting are formulated for further batches and physical characterization, in vitro drug release and in vivo studies are also carried out by using this drug to polymer ratio with 1% Poloxamer-188 concentration.

## RESULTS AND DISCUSSION

### Particle size and Zeta potential

The study of particle size is generally used as a characterization tool. Table 8 shows the particle size of the nanosuspension before and after Lyophilization, which shows a difference in particle size.

**Table 10: Particle Size data before and after Lyophilization.**

| The Ratio of Drug: Polymer with 1% Poloxamer -188 | Mean particle size (nm) before Lyophilization | Mean particle size (nm) after Lyophilization |
|---|---|---|
| 1: 10 | 133 ± 4.4 | 157 ± 4.2 |

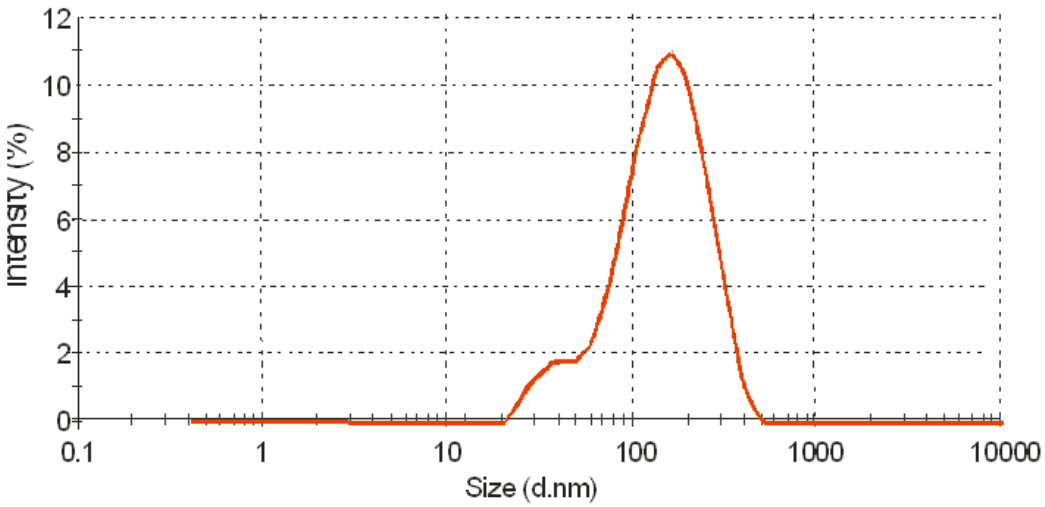


**Figure 7: Size analysis report of Risperidone: PLGA (1:10) nanoparticles (Before Lyophilization).**

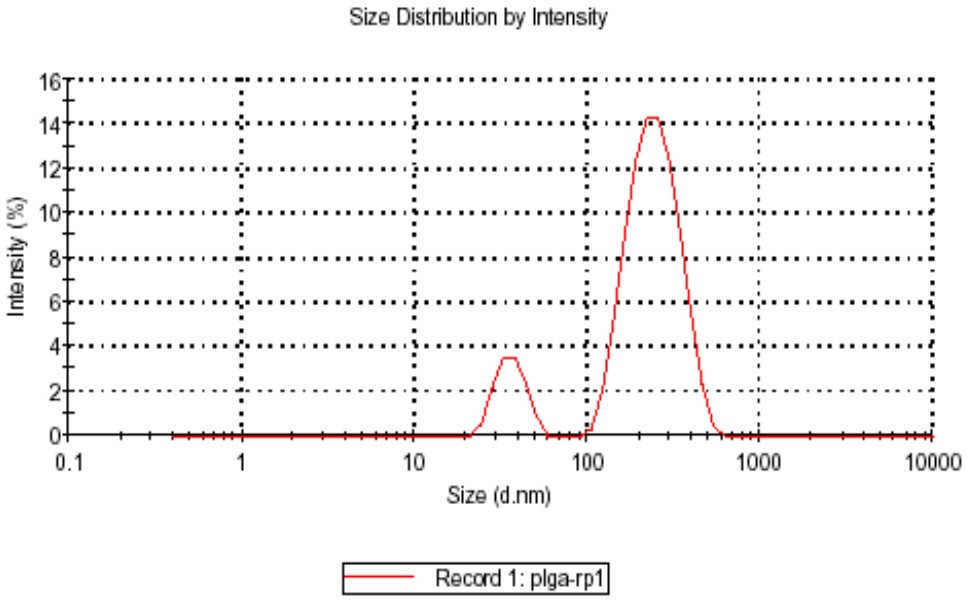


**Figure 8: Size analysis report of Risperidone: PLGA (1:10) nanoparticles (After Lyophilization)**

The increase in particle size of lyophilized nanoparticles might be due to the aggregation of PLGA nanoparticles during lyophilization. The Zeta-potential for the optimized batch was found to be -12.4 ± 1.8 mV.

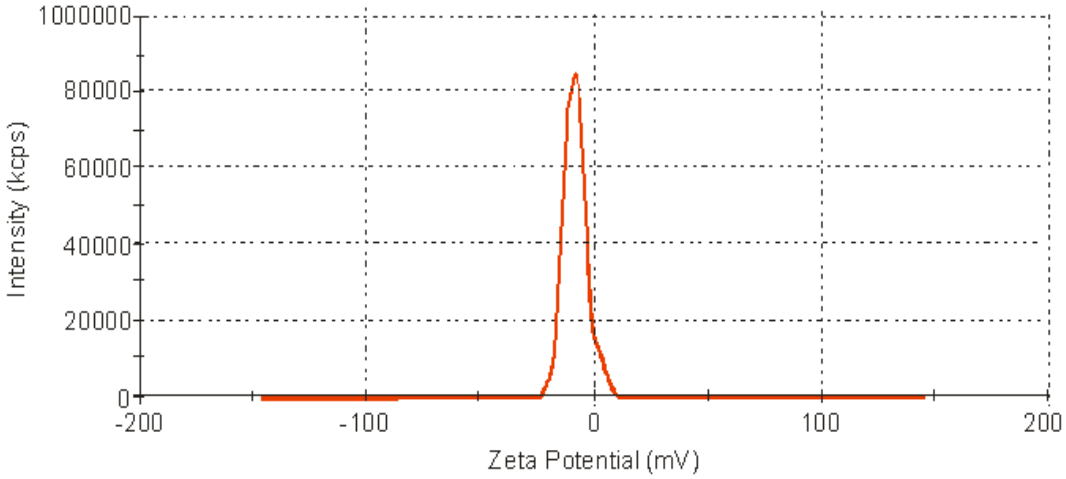


**Figure 9: Zeta potential of Risperidone: PLGA (1:10) nanoparticles.**

### 5.2.2 Entrapment Efficiency

Table 9 shows entrapment efficiency for the optimized batch. The entrapment efficiency was upto 89%.

**Table 11: Entrapment Efficiency for optimized batch.**

| Ratio of Drug: Polymer with 1% Poloxamer -188 | Entrapment Efficiency (%) |
|---|---|
| 1: 10 | 89.59 ± 3.21 |

### 5.2.3 Differential scanning calorimetry (DSC) Studies

Figure 5 shows Differential scanning calorimetry (DSC) of Risperidone, Poloxamer-188, PLGA 75:25, Placebo, and drug-loaded PLGA nanoparticles.

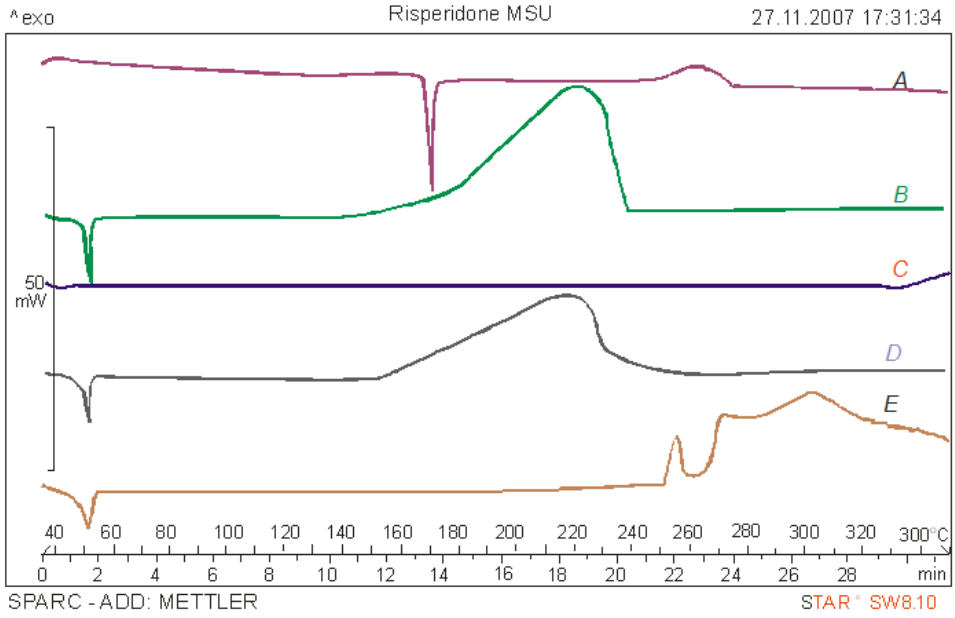


**Figure 10: DSC curve of Risperidone (A), Poloxamer-188 (B), PLGA 75:25 (C), Placebo (D) & drug-loaded PLGA nanoparticles (1:10) (E)**

The scan parameters of Risperidone, Poloxamer-188, Placebo & drug-loaded nanoparticles (1:10) presented in Table No.: 10, 11, 12, & 13 respectively.

**Table 12: Scan Parameters of Risperidone.**

| Pos. [°2Th.] | Height [cts] | FWHM [°2Th.] | d- spacing [A] | Rel. Int. [%] |
|---|---|---|---|---|
| 6.9408 | 197.42 | 0.0630 | 12.73592 | 2.62 |
| 10.5406 | 280.70 | 0.1102 | 8.39307 | 3.73 |
| 11.3265 | 630.03 | 0.1260 | 7.81236 | 8.37 |
| 13.6003 | 165.32 | 0.0945 | 6.51093 | 2.20 |
| 13.9145 | 1049.65 | 0.0945 | 6.336463 | 13.95 |
| 14.1311 | 3759.56 | 0.1260 | 6.26753 | 49.97 |
| 14.7372 | 1196.59 | 0.1260 | 6.01111 | 15.90 |
| 15.3905 | 456.41 | 0.1260 | 5.75740 | 6.07 |
| 16.3301 | 732.40 | 0.1102 | 5.42816 | 9.73 |
| 18.3936 | 1307.84 | 0.1417 | 4.8236 | 17.38 |
| 18.8323 | 2285.04 | 0.1102 | 4.71221 | 30.37 |
| 19.0878 | 245.30 | 0.1102 | 4.64970 | 3.26 |
| 19.6968 | 1820.06 | 0.1102 | 4.50731 | 24.19 |
| 21.1978 | 7523.58 | 0.1417 | 4.19140 | 100.00 |
| 22.0534 | 624.66 | 0.1260 | 4.03071 | 8.30 |
| 22.3793 | 1118.03 | 0.1574 | 3.97273 | 14.86 |
| 23.0882 | 2106.15 | 0.1417 | 3.85234 | 27.99 |
| 23.3898 | 634.43 | 0.1732 | 3.80334 | 8.43 |
| 24.2561 | 226.93 | 0.1260 | 3.66944 | 3.02 |
| 25.1240 | 311.28 | 0.1574 | 3.54461 | 4.14 |
| 25.2701 | 362.51 | 0.0787 | 3.52444 | 4.82 |
| 26.3365 | 75.94 | 0.1889 | 3.38410 | 1.01 |
| 27.4436 | 468.82 | 0.1260 | 3.25005 | 6.23 |
| 27.8125 | 171.77 | 0.0945 | 3.20777 | 2.28 |
| 28.2864 | 543.16 | 0.1574 | 3.15510 | 7.22 |
| 28.4389 | 518.83 | 0.0945 | 3.13853 | 6.90 |
| 28.8977 | 1519.91 | 0.1417 | 3.08937 | 20.20 |
| 29.4094 | 111.93 | 0.1574 | 3.03713 | 1.49 |
| 30.2259 | 112.06 | 0.2519 | 2.95692 | 1.49 |
| 32.3151 | 287.64 | 0.1574 | 2.77037 | 3.82 |
| 32.9475 | 337.89 | 0.0945 | 2.71863 | 4.49 |
| 33.5385 | 279.19 | 0.0945 | 2.67206 | 3.71 |
| 34.2139 | 91.19 | 0.2204 | 2.62084 | 1.21 |
| 35.2286 | 129.22 | 0.0945 | 2.54765 | 1.72 |
| 37.2357 | 138.13 | 0.1889 | 2.41480 | 1.84 |
| 38.4122 | 201.02 | 0.1574 | 2.34351 | 2.67 |

**Table 13: Scan Parameters of Poloxamer-188.**

| Pos. [°2Th.] | Height [cts] | FWHM [°2Th.] | d- spacing [A] | Rel. Int. [%] |
|---|---|---|---|---|
| 15.0789 | 80.60 | 0.1889 | 5.87532 | 2.75 |
| 19.1284 | 2765.80 | 0.1260 | 4.63993 | 94.97 |
| 21.1878 | 88.91 | 0.3779 | 4.19338 | 3.04 |
| 22.0657 | 257.25 | 0.1889 | 4.02848 | 8.79 |
| 23.0542 | 2377.48 | 0.2204 | 3.85795 | 81.21 |
| 23.3352 | 2927.68 | 0.1102 | 3.81211 | 100.00 |
| 26.2008 | 245.06 | 0.3779 | 3.40132 | 8.37 |
| 26.8275 | 240.34 | 0.3149 | 3.32328 | 8.21 |
| 27.8280 | 72.94 | 0.2519 | 3.20608 | 2.49 |
| 36.0893 | 187.86 | 0.4408 | 2.48884 | 6.42 |

**Table 14: Scan Parameters of Placebo.**

| Pos. [°2Th.] | Height [cts] | FWHM [°2Th.] | d- spacing [A] | Rel. Int. [%] |
|---|---|---|---|---|
| 15.1340 | 96.15 | 0.1102 | 5.85439 | 5.32 |
| 19.1507 | 1806.42 | 0.1732 | 4.63458 | 100.00 |
| 22.0471 | 180.22 | 0.2519 | 4.03183 | 9.98 |
| 23.4714 | 1607.85 | 0.1732 | 3.79030 | 89.01 |

| | | | | |
|---|---|---|---|---|
| 26.2065 | 155.01 | 0.5038 | 3.40060 | 8.58 |
| 26.8448 | 145.12 | 0.5038 | 3.32116 | 8.03 |
| 30.8262 | 47.34 | 0.3779 | 2.90070 | 2.62 |
| 35.4117 | 95.14 | 0.5038 | 2.53489 | 5.27 |
| 36.1439 | 123.65 | 0.3149 | 2.48520 | 6.84 |

**Table 15: Scan Parameters of Drug loaded PLGA Nanoparticles.**

| Pos. [°2Th.] | Height [cts] | FWHM [°2Th.] | d- spacing [A] | Rel. Int. [%] |
|---|---|---|---|---|
| 14.8621 | 45.44 | 0.7557 | 5.96087 | 4.95 |
| 19.1239 | 774.40 | 0.1102 | 4.64102 | 84.31 |
| 23.2272 | 918.52 | 0.2204 | 3.82958 | 100.00 |
| 26.2236 | 71.12 | 0.8817 | 3.39842 | 7.74 |
| 35.9987 | 51.25 | 0.5038 | 2.49489 | 5.58 |

XRD analysis was performed to confirm the results of DSC studies. In the x-ray diffractograms of Risperidone, sharp peaks at a diffraction angle (2θ) of 14.13°, 18.83°, 21.20°, 23.08°, and 28.89° indicate the presence of the crystalline drug. Poloxamer-188 shows broad peaks at 19.12° and 23.33°. No peak is observed in the XRD of PLGA 75:25 due to its polymeric nature. X-ray diffractogram of Placebo shows peaks at 19.08 and 23.47 with reduced height than X-ray diffractograms of Poloxamer-188. X-ray diffractogram of drug-loaded nanoparticles (1:10) shows peaks at 19.12° and 23.22° with a reduction in peak height. The above data reveal that the typical drug crystalline peaks were not detectable in drug-loaded nanoparticles (1:10). This finding confirms the dispersion of Risperidone at a molecular state within the nanoparticles.

**Scanning Electron Microscopy [SEM] Studies**

Figure 11, shows that SEM of Risperidone-loaded PLGA nanoparticles prepared with Poloxamer-188 as a surfactant are smooth and spherical in shape.

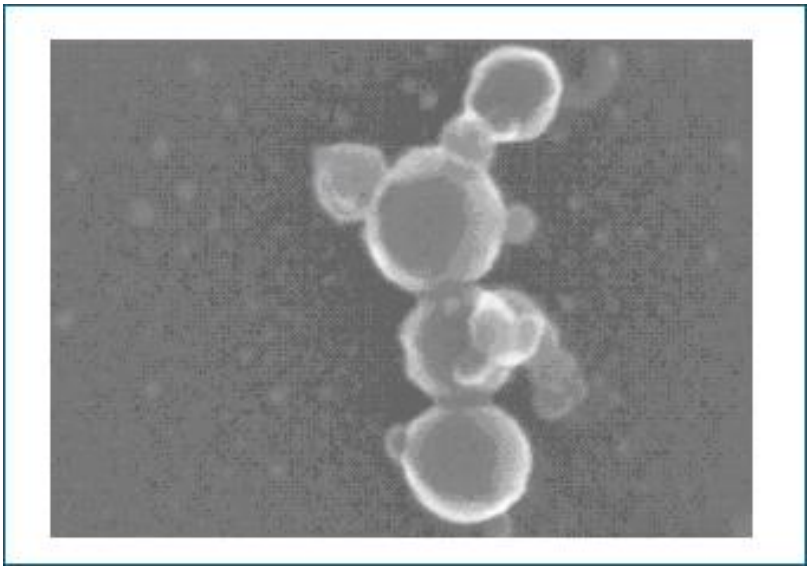

**Figure 11: Scanning Electron Microscopy [SEM] of PLGA nanoparticles.**

***In vitro* drug release Studies**

Table 16 shows in vitro drug release study of Risperidone-loaded PLGA nanoparticles with the different Drug: Polymer ratios by using 1% Poloxamer-188 as surfactant.

**Table 16: Drug release pattern for PLGA nanoparticles with different Drug to Polymer ratio.**

| Time [Hrs] | % Drug release [1:5] ratio | % Drug release [1:10] ratio | % Drug release [1:15] ratio |
|---|---|---|---|
| **1** | 33.48 | 3.48 | 0.6 |
| **6** | 65.87 | 12.7 | 4.8 |
| **12** | 87.85 | 29.34 | 15.6 |
| **24** | 92.46 | 39.06 | 22.08 |
| **48** | -- | 71.72 | 33.24 |
| **72** | --- | 89.25 | 45.87 |

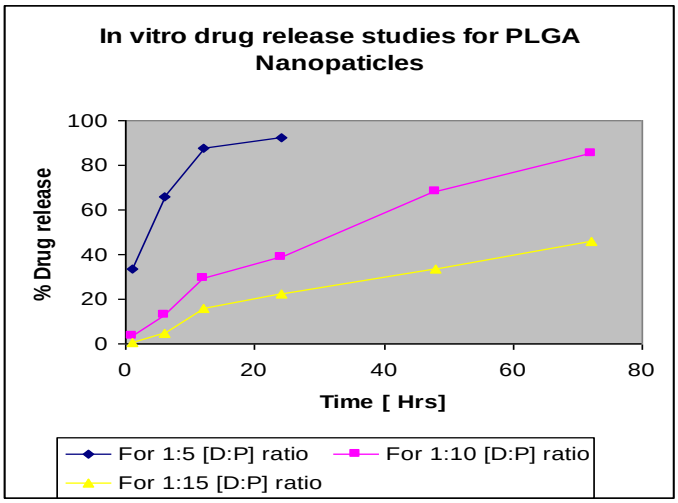


**Figure 12: Drug release pattern for PLGA nanoparticles with different Drug to Polymer ratio.**

Figure No. 12 shows, Risperidone-loaded PLGA Nanoparticles follow the Fickian pattern which releases 12.71% of the drug within 6 Hrs. from nanoparticles followed by 29.34% in 12 Hrs, 39.06% in 24 Hrs, 71.72% in 48 Hrs, and 89.25% in 72 Hrs. Thus, *in-vitro* drug release shows that a small portion of drug still present in the nanoparticles which could be released further. It signifies sustained release effect of formulation which in turn reduces frequency.

### *In Vivo* Radiolabelling and Biodistribution Studies

### Radiolabelling

The amount of stannous chloride added plays an important role in the labelling process. The influence of stannous chloride on the labelling efficiencies and the formation of colloids. A low amount of stannous chloride leads to poor labelling efficiencies because of insufficient reduction of pertechnetate to its lower valence state, whereas higher conc. of stannous chloride leads to the formation of undesirable radiocolloids.

The labelling efficiency and stability of the label complex were determined by using PC, TLC, and ITLC chromatography.

### Stability of $^{99m}$Tc labelled complex

In vitro serum stability of $^{99m}$Tc labelled complex of Risperidone was determined up to 24 Hrs by using acetone as a mobile phase.

**Table 17: Stability data of $^{99m}$Tc-radiolabelled complex in the human serum.**

| Hrs. | 50µlits [TLC] | 500µlits[TLC] | 50µlits[ITLC] | 500µlits[ITLC] |
|---|---|---|---|---|
| **1** | 99.75 | 99.85 | 99.70 | 99.85 |
| **2** | 99.45 | 99.60 | 99.65 | 99.67 |
| **4** | 98.98 | 98.45 | 98.64 | 98.75. |
| **8** | 98.60 | 98.37 | 98.54 | 98.38 |
| **24** | 97.35 | 97.67 | 97.64 | 97.55 |

The data shows that the labelled complex remained stable in serum up to a time period of 24 Hrs. The serum stability of the labelled complex indicates their use as potential marker for biodistribution studies.

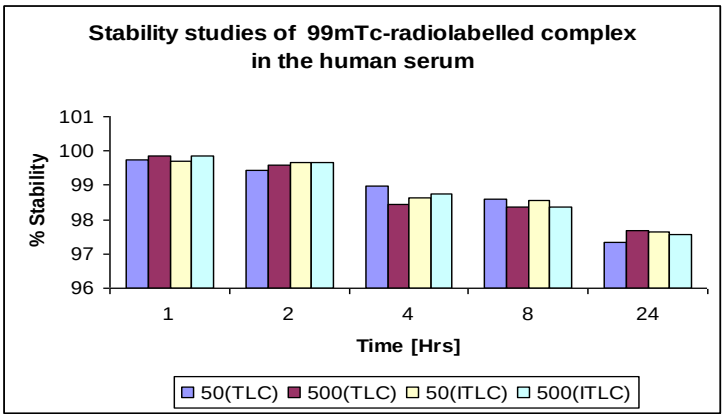


**Figure 13: Stability data of $^{99m}$Tc-radiolabelled complex in the human serum.**

**6.4.3 DTPA and Cysteine Challenging test**

DTPA and cysteine challenge studies were performed to obtain information on the transchelation (a measure of binding strength). Challenge studies demonstrated that the labelling efficiency of the complexes did not alter much in the presence of DTPA and cysteine. Even at a 100 mM concentration of DTPA and cysteine, the transchelation was found to be less than 5%, indicating the stability of the radiolabelled complexes.

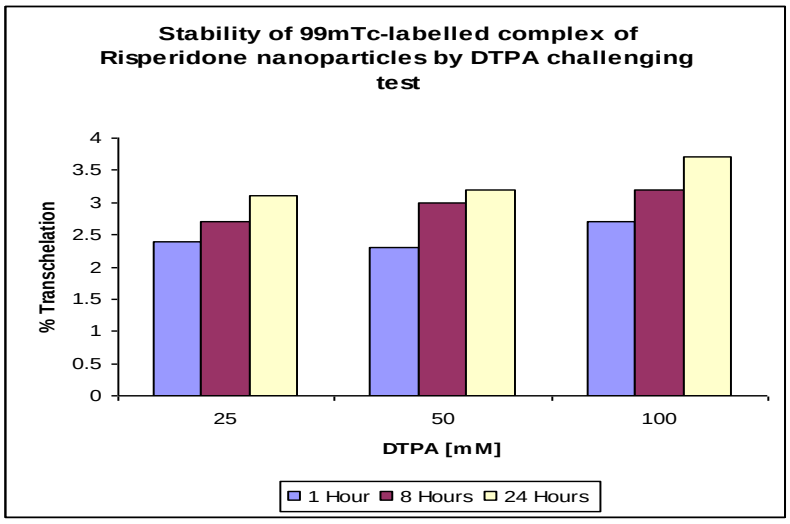


**Figure 14: *In vitro* stability of $^{99m}$Tc-labelled complex of Risperidone nanoparticles by DTPA challenging test.**

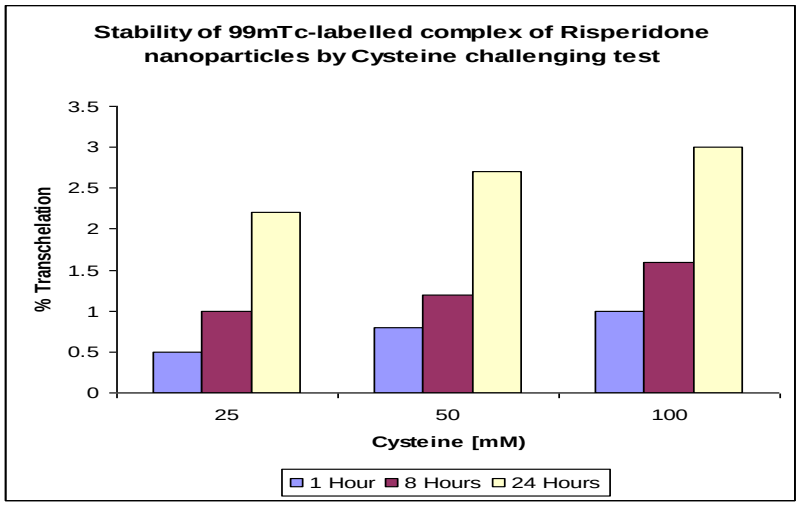


**Figure No 15: *In vitro* stability of $^{99m}$Tc-labelled complex of Risperidone nanoparticles by Cysteine Challenging test.**

**Biodistribution studies**

Plain Risperidone solution exhibit higher concentration in the organs like the reticuloendothelial system [RES uptake], such as the liver, spleen, and lung when compared to the Nanoparticulate system. The concentration of Risperidone-loaded nanoparticles concentration was found to be higher in blood for 1 hour and decreases with time which indicates the release of the drug from the systemic circulation to the target site. However, in kidneys, there was a gradual increase in the Risperidone conc. in both plain and nanoparticulate systems, as the kidney is the major metabolic site of Risperidone. The conc. of Risperidone in the brain was relatively 3-fold higher than plain Risperidone solution in 1 hour, followed by 3.2- fold in 4 hours and 4.91- fold higher after 12 hours. A small amount of radioactivity was also recovered from the stomach, intestine, and heart. The radioactivity in bone and muscles shows constancy with time indicating the in vivo stability of the radiolabelled complex. The increased brain concentration obtained in the Risperidone-loaded PLGA nanoparticles when compared to plain Risperidone is explained as follows: Poloxamer-188 acts as a surfactant and is also reported to inhibit the p-glycoprotein (p-gp) drug efflux system at the Blood-Brain Barrier which, ultimately causes the permeability of drugs across the Blood-Brain Barrier.

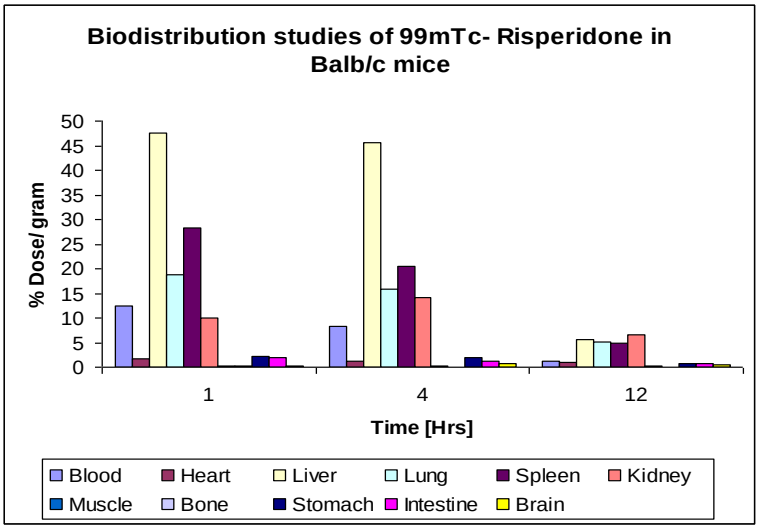


**Figure 16: Biodistribution studies of $^{99m}$ Tc- Risperidone in Balb/c mice.**

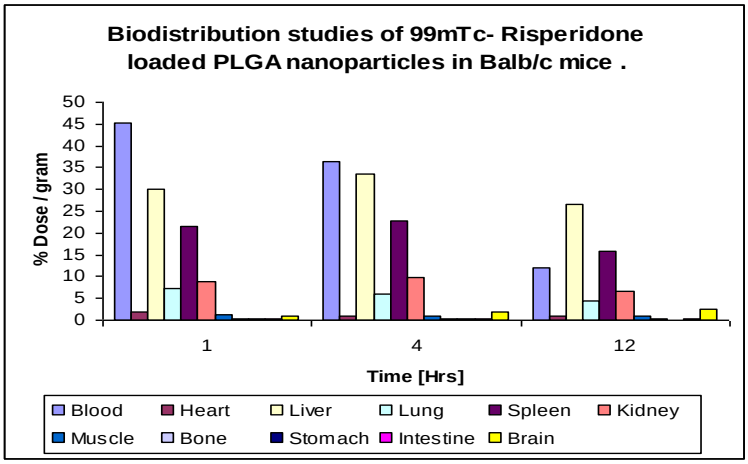


**Figure 17: Biodistribution studies of $^{99m}$ Tc- Risperidone-loaded PLGA nanoparticles in Balb/c mice.**

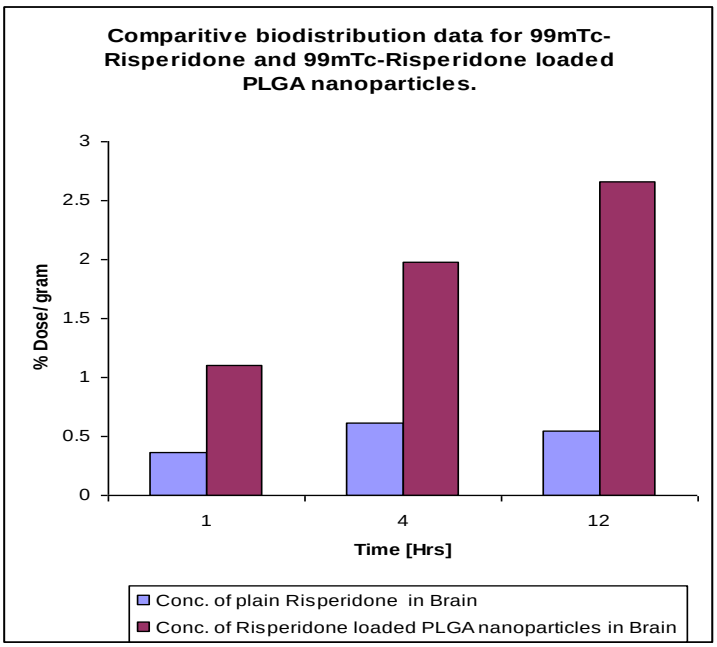


**Figure 18: Comparative biodistribution studies of $^{99m}$ Tc- Risperidone and $^{99m}$Tc- Risperidone-loaded PLGA nanoparticles in Balb/c mice.**

From this result, we can conclude that Risperidone-loaded PLGA nanoparticles cross the Blood-brain barrier more than plain Risperidone drugs and are also found to give sustained release activity.

## SUMMARY AND CONCLUSION

### Summary

The Blood-brain barrier is permeable to small and lipophilic (fat-loving) molecules (up to 800 atomic mass units, but larger molecules are not transported across unless there is an active transport system available. Thus, this is one of the stumbling blocks for drug delivery. An additional problem is the very effective efflux systems p-glycoprotein (p-gp), which pump the drug back out of cells. Overcoming, the difficulty of delivering therapeutic agents to specific regions of the brain presents a major challenge to the treatment of most brain disorders. In its neuroprotective role, the Blood-brain barrier functions to hinder the delivery of many potentially important diagnostic and therapeutic agents to the brain. Therapeutic molecules and genes that might otherwise be effective in diagnosis and therapy do not cross the Blood-brain barrier in adequate amounts. Nanomedical approaches to drug delivery center on developing nanoscale particles or molecules to improve the bioavailability of a drug. Nanoparticles drug carriers consist of solid biodegradable particles in sizes ranging from 10 to 1000 nm. They cannot freely diffuse through the Blood-brain barrier and require receptor-mediated transport through brain capillary endothelium to deliver their content into the brain parenchyma. Long-circulating nanoparticles made of methoxypoly (ethylene glycol) - polylactide or poly (lactide-co-glycolide) (mPEG-PLA/PLGA) has good safety profiles and provide drug-sustained release. Risperidone belongs to the second generation or atypical antipsychotic drug. This class of drug includes Risperidone, olanzapine, zyprasidone, quetiapine, aripiprazole and clozapine. The atypical antipsychotic drugs have advantages over traditional antipsychotics such as chlorpromazine and haloperidol. They selectively bind to central dopamine $D_2$ and (5-$HT_{2C}$) receptors and appear more effective in the symptoms of schizophrenia with less extrapyramidal symptoms. The overall goal of this research is to enhance the Risperidone concentration in the brain by administering the Risperidone-loaded biodegradable PLGA nanoparticles through the intravenous route. To provide the sustained release effect of the drug and also to reduce the frequency of administration of the drug.

### Analytical methods

The analytical method of Risperidone is done by using UV-spectrophotometer for the estimation of Risperidone in the formulation and diffusion media. The standard calibration curve of Risperidone was developed in 0.1N HCL, Acetone, Acetonitrile, and PBS buffer 7.4 at 288 nm and represented graphically. The developed analytical method was validated for accuracy, precision, and linearity.

### Formulation and optimization

Risperidone-loaded PLGA nanoparticles were prepared by the Solvent Displacement method or Nanoprecipitation Technique. 100 mg of PLGA 75:25 and 10 mg of Risperidone were dissolved in 5 ml of the solvent system [Acetone, Methanol, and Chloroform have been tried alternatively], which result in the formation of the organic phase. The aqueous phase was prepared by adding 0.1gm of Poloxamer-188 in distilled water [previously filter through 0.22µm]. Then the organic phase was injected into the aqueous phase at the rate of 0.3ml/min. and the stirring was allowed to continue for 3-4 Hrs for the complete removal of organic solvent. The Lyophilization of nanoparticles was carried out by adding sucrose as a cryoprotectant for 24 Hrs. The free drug was separated by using the Sephadex G-25 column.

Optimizations of nanoparticles were carried out for different solvent systems like acetone, methanol, and chloroform. At the same time, the drug to polymer ratio had optimized and formed that the optimized batches were carried out for a 1:10 drug to polymer ratio by using Poloxamer-188 as a surfactant. Optimizations of nanoparticles were also carried out for different surfactants with different conc. range. By using the Tween-80 as a surfactant the size of nanoparticles was found between 225 to276nm, which is not suitable for efficient brain targeting. At the same time, the entrapment efficiency was found in the range of 62.15% which was found to be very less for the nanoparticulate system. As the particle size was found to be above the optimization was further tried for Poloxamer-188 with different concentrations. Thus, by using different concentrations of poloxamer-188, the particle size was found in the range of 100 to 150 nm, with the highest entrapment efficiency. Hence, the further optimized batches were carried out by using the Drug: Polymer of 1:10 by using 1%w/v of Poloxamer-188 conc. The free drug was separated by using a Sephadex G-25 column and the entrapment efficiency was determined by lysis of nanoparticles in Acetonitrile at 278 nm, spectrophotometrically. At the same time particle size, polydispersity index, and Zeta-potential was measured. The entrapment efficiency of optimized batches was found in the range of 88.28 to 89.87%.

### Physical characterization of Risperidone-loaded PLGA nanoparticles

Physical characterization was carried out to optimized batches [1:10], Drug: Polymer ratio with 1% Poloxamer-188. The nanoparticle formulation was characterized for size, polydispersity index (PDI), Zeta-potential, entrapment efficiency, DSC, XRD, and SEM studies. The particle size of optimized batches was found in the range of 131 to 133 nm, with the entrapment efficiency found in the range of 88.28 to 89.87%. From the DSC curve of drug-loaded nanoparticles, the endothermic peak corresponding to the melting of Risperidone was absent. It might be due to the presence of Risperidone

dispersed at the molecular state within the nanoparticles. The DSC curve also shows the presence of merged endothermic peaks of Poloxamer-188 and PLGA 75:25 at 51.10°C and also decomposition peaks were also observed. The DSC study did not detect any crystalline drug peak in nanoparticle formulation. It concludes that Risperidone in the nanoparticles formulation was an amorphous or disperses in the polymer matrix. X-ray diffractogram of drug-loaded nanoparticles (1:10) shows peaks at 19.12° and 23.22° with a reduction in peak height. The above data reveal that the typical drug crystalline peaks were not detectable in drug-loaded nanoparticles (1:10). This finding confirms the dispersion of Risperidone at the molecular state within the nanoparticles. SEM of nanoparticles prepared with Poloxamer-188 as a surfactant were smooth and spherical in shape.

***In vitro drug* release**

In vitro, drug release studies of Risperidone from nanoparticles were determined using the Dialysis bag diffusion technique. The dialysis bag was immersed in the receptor compartment containing 60 ml of PBS (pH-7.4), maintained at $37^0$C. Samples were withdrawn at a regular interval throughout 72Hrs and assayed spectrophotometrically for drug content at 277 nm. The drug release profile shows that the release of drug from the nanoparticles followed the Fickian diffusion.

***In vivo* study**

**Radiolabelling of Nanoparticulate system**

*In vivo* study of Risperidone-loaded nanoparticles was done by Radiolabelling with $^{99m}$Tc. Risperidone-loaded PLGA Nanoparticles were radiolabelled with $^{99m}$Tc by using stannous chloride as a reducing agent. The Radiolabelling efficiency of Nanoparticles formulation was determined by instant ascending thin layer chromatography [ITLC], Paper chromatography [PC], and thin layer chromatography [TLC].

**Stability of $^{99m}$Tc labelled complex in Human serum**

The vitro stability of radiolabel complex in human serum was studied for 24 Hrs. at $37^0$ C. The samples were withdrawn at the regular interval up to 24 Hrs and analyzed by using ITLC, and radioactivity was measured by using a Scintillation counter. The data shows that the labelled complex remained stable in serum up to a time period of 24 Hrs.

**DTPA and cysteine challenging test**

These studies were performed in order to check the binding strength of $^{99m}$Tc with the radiolabelled complex. In brief, fresh solutions of DTPA and Cysteine (25, 50, and 100 mM) were prepared in 0.9% saline. The effect of DTPA and Cysteine on the labelling efficiency of complexes was measured by ITLC-silica gel strips using Pyridine: Acetic acid: Water [3: 5: 1.5] as the mobile phase. The data shows trans-chelation was found to be less than 5%, indicating the stability of the radiolabelled complexes.

**Biodistribution study**

Quantitative biodistribution studies were performed in Balb/c mice ~20 to 25gm. The biodistribution studies of radiolabelled complex Risperidone nanoparticles were performed after 1 hour, 4 hours, and 12 hours of post-injection. Unanaesthetised animals were injected with the $^{99m}$Tc-labelled complex of Risperidone-loaded nanoparticles via the tail vein. After 1 hour, 4 hours, and 12 hours animals were anesthetized with chloroform and at these time intervals, the blood was collected by cardiac puncture and sacrificed by decapitation. The organs were then weighed and measured for radioactivity in a gamma ray spectrometer. Plain Risperidone solution exhibit higher concentration in the organs like the reticuloendothelial system [RES uptake], such as the liver, spleen, and lung when compared to the Nanoparticulate system. The concentration of Risperidone-loaded nanoparticles concentration was found to be higher in blood for 1 hour and decreases with time which indicates the release of the drug from the systemic circulation to the target site. However, in the kidney, there was a gradual increase in the Risperidone concentration in both the plain and nanoparticulate system, as the kidney is a major metabolic site of Risperidone. The concentration of Risperidone in the brain was relatively 3-fold higher than plain Risperidone solution in 1 hour, followed by 3.2- fold in 4 hours and 4.91- fold higher after 12 hours.

From this result, we can conclude that Risperidone-loaded PLGA nanoparticles cross the Blood-brain barrier more than plain Risperidone drugs and were also found to give sustained release activity.

## CONCLUSIONS

Risperidone-loaded PLGA nanoparticles were developed and optimized by the Nanoprecipitation technique. Analytical methods were developed for the estimation of Risperidone in the nanoparticulate system. The nanoparticle formulation was characterized for particle size, P.D.I, Zeta-potential, Entrapment efficiency, DSC, XRD, SEM, and in vitro drug release studies, which reveals the formation of Risperidone-loaded nanoparticles with release profile. In vivo, a biodistribution study of Risperidone-loaded nanoparticles was done by Radiolabelling with $^{99m}$Tc in Balb/c mice. The following significant conclusions were obtained from the above result:

1. Poly (lactic-co-glycolide) 75:25 can incorporate highly lipophilic drugs like Risperidone, olanzapine, and ziprasidone.
2. Risperidone-loaded PLGA nanoparticles were prepared by the Nanoprecipitation technique to obtain the particle size below 150 nm with high entrapment efficiency found in the range of 88.28 to 89.87 %.
3. DSC, XRD, SEM, and in vitro drug release studies, reveal the formation of Risperidone-loaded nanoparticles with release profile.

4. From the in vivo biodistribution study of Risperidone-loaded PLGA nanoparticles with $^{99m}$Tc in Balb/c mice concluded that nanoparticles prepared with a 1:10 ratio of Risperidone: PLGA [75:25] with 1%w/v of Poloxamer-188 concentration, shows significantly higher brain concentration of drug as compared to plain drug solution with sustained drug release activity.

Thus, it concludes, that Risperidone-loaded PLGA nanoparticles provide higher drug concentration in the brain with sustained drug release activity.

## LIST OF ABBREVIATION

PLGA: poly D, L-lactic-co-glycolic acid
Blood-Brain Barrier: BBB
UCLA: University of California, Los Angeles
nm: Nanometer
%: Percent
PLA NP: Poly-lactic acid nanoparticles
IV: Intravenous
µm: Micrometer
CNS: central nervous system
FDA: Food and Drug Administration
$T_g$: Glass transition temperature
°C: Degree Celsius
dL/g**:** Deciliters per gram
g/ml: Gram per milliliter
PEG: Polyethylene Glycol
GMP: Good manufacturing practice
NPs: Nanoparticles
PVA: Polyvinyl alcohol
mg: milligram
g: Gram
ml: Milliliter
RPM: Revolutions per minute
Hrs: Hours
µlits: microliter
cm: centimeter
Min: Minutes
mM: Millimeter
mV: Mean diameter
P.D.I: Polydispersity index

## CONFLICTS OF INTEREST

The authors declare no conflict of interest.

## ACKNOWLEDGEMENTS

I would like to express my great appreciation to Dr. Abhay Dharamsi, Dean and Principal, Parul Institute of Pharmacy, Parul University., for his valuable and constructive suggestions during the planning and development of this research work.

## REFERENCES

1. Flashman LA, Green MF. Review of cognition and brain structure in schizophrenia: profiles, longitudinal course, and effects of treatment. Psychiatr Clin North Am, 2004; 27(1): 1-18.
2. W Rhodri, Schizophrenia: A cyclical and heterogeneous dysfunction of cognitive and sensory processing, Psychopathology, 1999; 112: 185-189.
3. Chen Y, Dalwadi G, Benson H. Drug delivery across the Blood-Brain Barrier. Curr. Drug Deliv, 2004; 1(4): 361-76.
4. Allen TM, Cullis PR. Drug delivery systems: entering the mainstream. Science, 2004; 303(5665): 1818-22.
5. Freitas RA. Current status of nanomedicine and medical nanorobotics. J. Comput. Theor. Nanosci, 2005; 2(1): 1-25.
6. Bertelsen A. Schizophrenia and related disorders: experience with current diagnostic systems. Psychopathology, 2002; 35(2-3): 89-93.
7. P Ehrlich, Collected Studies on Immunity. 1st ed. J. Wiley & Sons, New York, 1906; 586.
8. Elias Fattal Christine Vauthier, Drug Delivery: Nanoparticles, in Encyclopaedia of Pharmaceutical Technology, J Swarbrick, Marcel Dekker Inc., New York, USA, 1994; 165-90.
9. Barratt GM. Therapeutic applications of colloidal drug carriers. Pharm. sci. technol. Today, 2000; 3(5): 163-71.
10. RJ Linhardt, Biodegradable polymers for controlled release of drugs, M Rosoff Editor, 1989, New York VCH Publishers, 53– 95.
11. Desai MP, Labhasetwar V, Walter E, Levy RJ, Amidon GL. The mechanism of uptake of biodegradable microparticles in Caco-2 cells is size dependent. Pharm. Res., 1997; 14(11): 1568-73.
12. Wang C, Shim M, Guyot-Sionnest P. Electrochromic nanocrystal quantum dots. Science, 2001; 291(5512): 2390-2.
13. Chen Y, Dalwadi G, Benson H. Drug delivery across the Blood-Brain Barrier. Curr. Drug Deliv, 2004; 1(4): 361-76.
14. Panyam J, Labhasetwar V. Biodegradable nanoparticles for drug and gene delivery to cells and tissue. Adv. Drug Deliv. Rev., 2003; 55(3): 329-47.
15. Wu L, Ding J. In vitro degradation of three-dimensional porous poly (D, L-lactide-co-glycolide) scaffolds for tissue engineering. Biomaterials, 2004; 25(27): 5821-30.
16. Astete CE, Sabliov CM. Synthesis and characterization of PLGA nanoparticles. J. Biomater. Sci. Polym. Ed., 2006; 17(3): 247-89.
17. Govender T, Stolnik S, Garnett MC, Illum L, Davis SS. PLGA nanoparticles prepared by nanoprecipitation: drug loading and release studies of a water soluble drug. JCR., 1999; 57(2): 171-85.
18. Blasi P, D'Souza SS, Selmin F, DeLuca PP. Plasticizing effect of water on poly (lactide-co-glycolide). JCR., 2005; 108(1): 1-9.
19. Prabha S, Labhasetwar V. Critical determinants in PLGA/PLA nanoparticle-mediated gene expression. Pharm. Res., 2004; 21(2): 354-64.
20. Blasi P, D'Souza SS, Selmin F, DeLuca PP. Plasticizing effect of water on poly (lactide-co-glycolide). JCR., 2005; 108(1): 1-9.

21. Jeong B, Bae YH, Lee DS, Kim SW. Biodegradable block copolymers as injectable drug-delivery systems. Nature, 1997; 388(6645): 860-2.
22. Ikada Y, Tsuji H. Biodegradable polyesters for medical and ecological applications. Macromolecular rapid communications, 2000; 21(3): 117-32.
23. Jeong B, Bae YH, Kim SW. Drug release from biodegradable injectable thermosensitive hydrogel of PEG–PLGA–PEG triblock copolymers. JCR., 2000; 63(1-2): 155-63.
24. Mundargi RC, Babu VR, Rangaswamy V, Patel P, Aminabhavi TM. Nano/micro technologies for delivering macromolecular therapeutics using poly (D, L-lactide-co-glycolide) and its derivatives. JCR., 2008; 125(3): 193-209.
25. Mundargi RC, Babu VR, Rangaswamy V, Patel P, Aminabhavi TM. Nano/micro technologies for delivering macromolecular therapeutics using poly (D, L-lactide-co-glycolide) and its derivatives. JCR., 2008; 125(3): 193-209.
26. Niwa T, Takeuchi H, Hino T, Nohara M, Kawashima Y. Biodegradable submicron carriers for peptide drugs: Preparation of dl-lactide/glycolide copolymer (PLGA) nanospheres with nafarelin acetate by a novel emulsion-phase separation method in an oil system. Int. J. Pharm., 1995; 121(1): 45-54.
27. Barrera DA, Zylstra E, Lansbury Jr PT, Langer R. Synthesis and RGD peptide modification of a new biodegradable copolymer: poly (lactic acid-co-lysine). JACS., 1993; 115(23): 11010-1.
28. Song C, Labhasetwar V, Murphy H, Qu X, Humphrey W, Shebuski R, et al. Formulation and characterization of biodegradable nanoparticles for intravascular local drug delivery. JCR., 1997; 43(2-3): 197-212.
29. Ruan G, Feng S-S. Preparation and characterization of poly (lactic acid)–poly (ethylene glycol)–poly (lactic acid) (PLA–PEG–PLA) microspheres for controlled release of paclitaxel. Biomaterials, 2003; 24(27): 5037-44.
30. Bilati U, Allemann E, Doelker E. Sonication parameters for the preparation of biodegradable nanocapsules of controlled size by the double emulsion method. Pharm. Dev. Technol, 2003; 8(1): 1-9.
31. Fessi H, Puisieux F, Devissaguet JP, Ammoury N, Benita S. Nanocapsule formation by interfacial polymer deposition following solvent displacement. Int. J. Pharm, 1989; 55(1): R1-R4.
32. Bindschaedler, Christian. EP PCT/EP88/00281, 1993.
33. Dong Y, Feng S-S. Methoxy poly (ethylene glycol)-poly (lactide) (MPEG-PLA) nanoparticles for controlled delivery of anticancer drugs. Biomaterials, 2004; 25(14): 2843-9.
34. Chattopadhyay P, Gupta RB. Protein nanoparticle formation by supercritical antisolvent with enhanced mass transfer. AIChE Journal, 2002; 48(2): 235-44.
35. Shekunov BY, Chattopadhyay P, Seitzinger J, Huff R. Nanoparticles of poorly water-soluble drugs prepared by supercritical fluid extraction of emulsions. Pharm. Res., 2006; 23(1): 196-204.
36. Tosi G, Costantino L, Rivasi F, Ruozi B, Leo E, Vergoni AV, et al. Targeting the central nervous system: in vivo experiments with peptide-derivatized nanoparticles loaded with Loperamide and Rhodamine-123. JCR., 2007; 122(1): 1-9.
37. J Kahn and B Kahn, Radioisotopes to Medical Imaging, History of Nuclear Medicine, Written at Berkeley, September 9, 1996. https://www2.lbl.gov/Science-Articles/Archive/nuclear-med-history.html
38. TF Budlinger, Attribute to single photon tomography, J. of nuclear medicine, California, 1980; 21: 579.
39. H Aoki and K Fuji, Radioisotopes in Medicine: Nuclear Issues Briefing, J. of nuclear medicine, January 2008; 241-252.
40. G Konrad, V Schulthess, Molecular Anatomic Imaging: PET-CT and SPECT-CT Integrated Modality Imaging, 2nd ed., Philadelphia; Lippincott Williams & Wilkins, 568 – 577.
41. N Ramamoorthy, CN Desai, Manual for accreditation programme for hospital radio pharmacist, Radio pharmacy practices in India, 1997; 1- 46.
42. Mra Pillai and N Ramamoorthy, Lecture notes for INCAS workshops, Bhabha Atomic research centre [BARC] Trombay.
43. La Bella R, Garcia-Garayoa E, Langer M, Blauenstein P, Beck-Sickinger AG, Schubiger PA. In vitro and in vivo evaluation of a $^{99m}$Tc (I)-labelled bombesin analogue for imaging of gastrin releasing peptide receptor-positive tumors. Nucl. Med. Biol., 2002; 29(5): 553-60.
44. Reddy LH, Sharma RK, Chuttani K, Mishra AK, Murthy RR. Etoposide-incorporated tripalmitin nanoparticles with different surface charge: formulation, characterization, Radiolabelling, and biodistribution studies. The AAPS journal, 2004; 6(3): 55-64.
45. Wunderlich G, Grüning T, Paulke B-R, Lieske A, Kotzerke J. $^{99m}$Tc labelled model drug carriers-labelling, stability and organ distribution in rats. Nuclear medicine and biology, 2004; 31(1): 87-92.
46. Lima MdJdC, Marques FLN, Okamoto MRY, Garcez AT, Sapienza MT, Buchpiguel CA. Preparation and evaluation of modified composition for lyophilized kits of [Cu (MIBI) 4] BF4 for [$^{99m}$Tc] technetium labelling. Braz. Arch. Biol. Technol, 2005; 48(SPE2): 1-8.79.